NeuroImage 61 (2012) 342–362

Contents lists available at SciVerse ScienceDirect

NeuroImage

journal homepage: www.elsevier.com/locate/ynimg

Review

The neurochemical profile quantified by *in vivo* ^{1}H NMR spectroscopy

João M.N. Duarte [a,b,*], Hongxia Lei [a,c], Vladimír Mlynárik [a], Rolf Gruetter [a,b,c]

[a] *Laboratory for Functional Metabolic Imaging, Ecole Polytechnique Fédérale de Lausanne, Switzerland*
[b] *Department of Radiology, University of Lausanne, Switzerland*
[c] *Department of Radiology, University of Geneva, Switzerland*

ARTICLE INFO

Article history:
Accepted 15 December 2011
Available online 28 December 2011

Keywords:
Neurochemical profile
NMR spectroscopy
Brain

ABSTRACT

Proton NMR spectroscopy is emerging from translational and preclinical neuroscience research as an important tool for evidence based diagnosis and therapy monitoring. It provides biomarkers that offer fingerprints of neurological disorders even in cases where a lesion is not yet observed in MR images. The collection of molecules used as cerebral biomarkers that are detectable by ^{1}H NMR spectroscopy define the so-called "neurochemical profile". The non-invasive quality of this technique makes it suitable not only for diagnostic purposes but also for therapy monitoring paralleling an eventual neuroprotection. The application of ^{1}H NMR spectroscopy in basic and translational neuroscience research is discussed here.

Contents

Abbreviations: AD, Alzheimer's disease; ALS, amyotrophic lateral sclerosis; BOLD, blood-oxygen-level dependence; CNS, central nervous system; CSI, chemical shift imaging; CRLB, Cramér-Rao lower bound; fMRI, functional MRI; GABA, γ-aminobutyrate; Glx, glutamate plus glutamine; GPC, glycerylphosphorylcholine; GSH, glutathione; HD, Huntington's disease; MRI, magnetic resonance imaging; MRS, magnetic resonance spectroscopy; NAA, *N*-acetylaspartate; NAAG, *N*-acetylaspartylglutamate; NMDA, *N*-methyl-D-aspartate; NMR, nuclear magnetic resonance; PCho, phosphorylcholine; PD, Parkinson's disease; PE, phosphorylethanolamine; PET, positron emission tomography; SCA1, spinocerebellar ataxia type 1; TCA, tricarboxylic acid; VOI, volume of interest; OVS, outer volume suppression; SAR, specific absorption rate; AFP, adiabatic-full-passage; AHP, adiabatic-half-passage; RF, radiofrequency; TE, echo time; TR, repetition time; SNR, signal-to-noise ratio; 3NP, 3-nitropropionic acid; BBB, blood-brain-barrier.

* Corresponding author at: EPFL SB IPMC LIFMET, (Bâtiment CH), Station 6, CH-1015 Lausanne, Switzerland.
E-mail address: joao.duarte@epfl.ch (J.M.N. Duarte).

1053-8119/$ – see front matter © 2011 Elsevier Inc. All rights reserved.
doi:10.1016/j.neuroimage.2011.12.038

Introduction

Enormous advances are occurring in the elucidation of the pathogenesis of neurological disorders. Their genetic characterization and the creation of transgenic mice developing human-like phenotypes of neuropathologies and neurodegeneration have greatly contributed in the effort for revealing the biochemical mechanisms of disease development and progression. We have now reached the moment when diagnostic tools are required to be reliable, applicable in a non-invasive way and to make a bridge between the clinical application and basic research. ^{1}H NMR spectroscopy is a potentially valuable, if not the best candidate to fulfill this role, since it allows monitoring brain neurochemistry in humans and animal models of neurological disorders in a non-invasive way, thus applicable longitudinally to monitor degeneration during disease progression or recession upon effective therapeutic intervention. Since exactly the same methodology can be applied to the human and to laboratory animals, it can be translated to the clinical routine. However, ^{1}H NMR spectroscopy of the rodent brain is technically challenging. These challenges of spectroscopy in rodents and particularly in mice had to be overcome to obtain reliable and quantifiable data. The small size of the animal's head implies that the region of interest for the NMR measurement is typically close to the interface between the diamagnetic tissue and the paramagnetic oxygen in air, thus inducing strong B_0 inhomogeneity. Efficient minimization of B_0 inhomogeneity (shimming) is required to achieve increased spectral resolution. Macroscopic susceptibility effects in different regions of the rodent brain can be eliminated with the use of contemporary shim coil designs for high order shimming. The inherently small size of the region of interest is further reduced when one aims to localize the spectra not only within the brain but to functionally different cerebral areas, thus reducing sensitivity that is the main intrinsic challenge of NMR spectroscopy. Sensitivity can, however, be optimized using for example quadrature surface coils for signal reception rather than using a transceiver

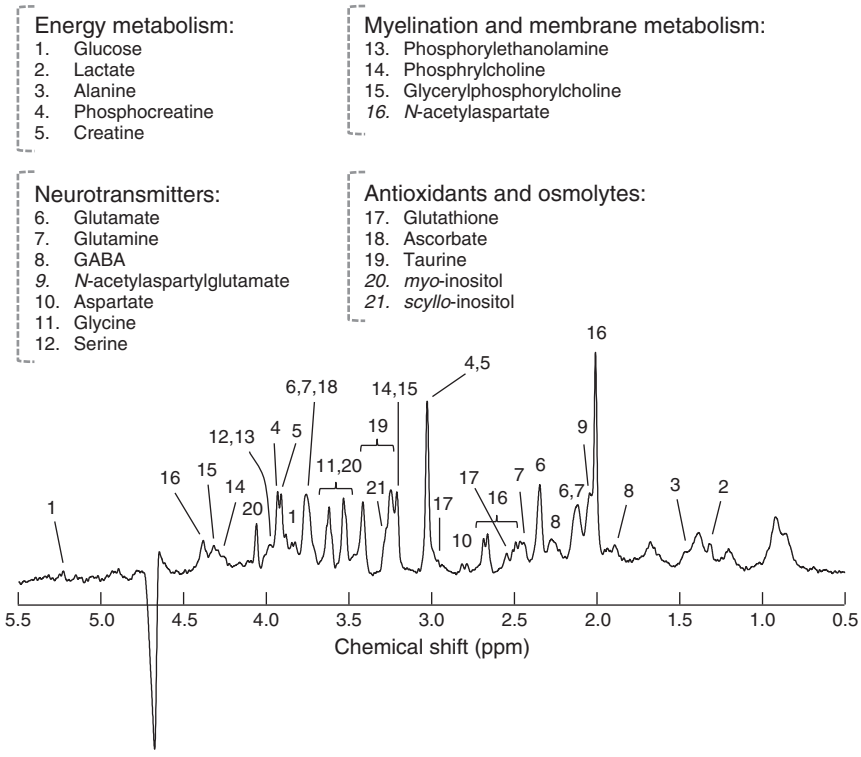

Fig. 1. Compounds detected in the brain with *in vivo* ^{1}H NMR spectroscopy. Spectrum was acquired from the rat hippocampus at 14.1 T using SPECIAL.

volume coil, which is characterized by sensitivity losses due to the small filling factor of the rodent brain. In addition, high magnetic fields and short echo times in carefully designed pulse sequences substantially improve sensitivity, as will be discussed bellow.

For a long time, ^{1}H NMR spectroscopy *in vivo* was performed with rather long echo times, simplifying the spectral analysis at low magnetic fields but allowing quantification of only few metabolites. Increases in sensitivity and spectral resolution at high magnetic fields provides an opportunity of quantifying at least 18 metabolites (Fig. 1) in the rodent brain at ultra-short echo time (Pfeuffer et al., 1999). Since then, *in vivo* ^{1}H NMR spectroscopy has been routinely used in preclinical and clinical research as well as continuously improved.

The present review article covers, first the technological aspects of NMR spectroscopy aiming at the acquisition of ^{1}H NMR spectra with sufficient quality for reliable quantification of an extended neurochemical profile. A second part of the review describes the relevance of the quantified metabolites for brain function. At last, disease applications of ^{1}H NMR spectroscopy and future directions are discussed.

In general, previous articles aiming at reviewing the *in vivo* usage of NMR spectroscopy for metabolite quantification described possible or plausible functions for the normally observed metabolites. Because each detected molecule is involved in different metabolic pathways and specific cerebral functions, in the present review we suggest that the inverse approach, i.e. a discussion of metabolites involved in each specific cellular role, should be preferred when probing the neurochemical profile. Therefore, for different functional aspects of the brain, the roles of different molecules are described and discussed within the metabolic network and not as isolated chemicals in test-tube environment.

Instrumentation for MR spectroscopy

To perform *in vivo* ^{1}H MR studies, a magnet, three orthogonal magnetic field gradients, a set of shim gradients, transmit/receive RF coils or a transceiver one, an RF amplifier, a transmit–receive switch, a preamplifier, a receiver (including analog–digital-convertors, ADC) and an interfaced console allowing the control of all hardware components are necessary. A full review of NMR instrumentation is beyond the scope of this review, see (e.g. de Graaf, 2008). MR detectable signals are induced by a train of radiofrequency (RF) pulses applied with or without gradients, received, amplified and saved for further analysis.

Before MRI was introduced, NMR spectroscopy (MRS) had been widely used in chemistry or physics. Thereafter, MRS, especially ^{1}H MRS, became an alternative means for *in vivo* studying brain function and diseases of human and animals. With increased strength and stability of magnets and availability of contemporary techniques, quality of *in vivo* ^{1}H NMR spectra has been markedly improved.

Strengths of magnets

The sensitivity of the MR measurement is enhanced by increasing magnetic field strength, i.e. SNR or $(\text{Signal}/\sigma_N) \propto B_0^{\beta}$ (Hoult and Richards, 1976). When signal (S) theoretically increases with B_0^2 and achievable sensitivity is exclusively due to an increase in B_0, β should be no more than 2. Taking into account only electric components and the RF coils as the dominant source of noise (N_e), its root-mean-square amplitude may increase with the square root of frequency (B_0). Consequently, the standard deviation of the random noise, σ_N, is the fourth root of B_0. This leads to a generally accepted $\beta = 1.75$. However, for *in vivo* spectroscopy, the sample becomes one major source of noise (N_s), which increases with B_0^2. Thus the increased sensitivity with B_0 is close to linearity, $\beta \sim 1$. Since the total noise is a combination of both components, i.e. $\sigma_N = \sqrt{(\sigma_{Ne}^2 + \sigma_{Ns}^2)/2}$ (when including both electrical and sample sources of noise), *in vivo* β is in the range of 1 to 1.75. Besides the noise, linewidths and relaxation times can influence sensitivity. At high magnetic field, not only magnetic susceptibilities but also longitudinal relaxation times increase. Recent studies at high magnet fields (i.e. above 9.4 T) reported T_1 of metabolites increased modestly (Cudalbu et al., 2009; de Graaf et al., 2006). Therefore, the sensitivity decrease due to an increase of T_1 is not substantial. In contrast, the T_2^* decrease markedly affects peak heights due to amplified susceptibility effects and reduction of transverse relaxation times (T_2) will diminish the sensitivity when measured at long echo times (Mekle et al., 2009; Tkáč et al., 2009).

Thus, the acquisition time at higher magnetic fields necessary for achieving a required SNR is shorter than those at lower fields. Shorter acquisitions allow functional MRS (fMRS) studies in both human (Mangia et al., 2007) and rodent brain (Xu et al., 2005). Additionally, spectral resolution is amplified with increased B_0. This considerably improves information content of ^{1}H MRS by reducing signal overlap, typically observed at lower magnetic fields (Mekle et al., 2009; Mlynárik et al., 2008a; Tkáč et al., 2009). With such advantages of high magnetic fields, studying the regional neurochemical profile in small volumes of mouse brain after various forms of intervention is feasible (Berthet et al., 2009, 2011; Lei et al., 2009).

Gradient performance

Non-invasive localization of the MR signal in the brain cannot be done without a magnetic field gradient system. The gradient system allows adding a magnetic field increasing or decreasing linearly along any of the three main axes of the coordinate system (G, mT/m). Then, the resulting magnetic field at a position r is $B(r) = B_0 + rG$. As a result, the resonance frequency becomes dependent on position r, $\omega(r) = \gamma B_0 + \gamma rG$. The performance of gradients is crucial for the quality of localized spectroscopy.

When the gradients are switched on and off, eddy currents are induced in conductors in the vicinity of gradient coils, which may potentially distort signals and induce localization errors that cause artifacts in both images and spectra. Active shielding of gradients reduces eddy currents substantially (Bowtell and Mansfield, 1991; Mansfield and Chapman, 1986; Turner et al., 1988) and in combination with effective compensation methods (Boesch et al., 1991; Jehensen et al., 1990; Kickler et al., 2010; Terpstra et al., 1998a; Van Vaals and Bergman, 1990) the eddy current effects can be minimized.

RF considerations

It is desirable to have a homogenous RF field covering the entire volume of interest (VOI) for both MR imaging and spectroscopy. In general, brain imaging is usually performed with volume RF coils, which are available for conventional MR scanners and provide sufficiently homogenous RF fields. However, when compared to the surface coils, volume coils require increased RF power owing to large volume coverage (Hoult and Richards, 1976). Conversely, increased power indicates diminished sensitivity based on the reciprocity principle. A potential risk of the increased power to an MR examination is that the RF energy is absorbed by the tissue and then converted to heat. Thus, the rate of energy absorption, the specific absorption rate (SAR), must be restricted in humans. With increased B_0, RF wavelengths are shortened and thus the RF field generated by a classic human volume transmit coil varies over space (so-called “dielectric resonance”). Although these problems can complicate imaging techniques at high magnetic fields, including MR spectroscopic imaging, use of adiabatic RF pulses and other alternatives offered intriguing ameliorations (Adriany et al., 2008; Avdievich et al., 2010; Henning et al., 2008; Hetherington et al., 2010; Katscher et al., 2003, 2005; Van de Moortele et al., 2005). On the other hand, for localized ^{1}H NMR spectroscopy, the RF field for the targeting volume can be calibrated using typically the tissue water signal. Recent human

studies showed that ^{1}H MRS of deep brain region is feasible using volume coil, while SAR is not of concern (Boer et al., 2011; Oz and Tkáč, 2011; Oz et al., 2006). However, when long RF trains are applied, such as broadband RF pulses for outer volume suppression, these limits can be exceeded.

In rodents, SAR concerns do not apply. The brain only occupies a very small portion of the head, thus the volume coil can be used as a transmitter producing a fairly homogeneous RF field. However, the MRS signal should be detected by a more sensitive surface coil. Alternatively, surface coils can be used as transceivers along with optimal adiabatic RF pulses, which can overcome problems arising from inhomogeneous RF fields. Numbers of studies have shown excellent performance of surface coils for NMR spectroscopy at high magnetic fields in rodent brain (Lei et al., 2010a,b; Tkáč et al., 1999), even for chemical shift imaging (Mlynárik et al., 2008a), as well as for high resolution EPI images with a full brain coverage (Lei et al., 2008; van de Looij et al., 2011b).

Coils at low temperature, cryo-coils, may provide gains in sensitivity by reducing the ohmic losses for both imaging (Ginefri et al., 2007; Kwok and You, 2006; Ma et al., 2003; Wright et al., 2000) and spectroscopy (Ratering et al., 2008). The SNR was doubled when comparing with the same coils at room temperature. This approach is very effective when the coil is the major source for noise, at the cost of increased distance between the coil and the sample due to the thermal isolation layer. For human subjects, as well as many rodent applications, the sample itself likely is the dominating contributor of noise. Therefore, the improvements due to using cryo-coils for these studies might be limited.

Field homogeneity

The sensitivity improvements achievable at high magnetic fields described above would not be possible unless the high magnetic field in the measured region is homogeneous enough. Magnetic field inhomogeneities can have a dramatic effect on the quality of spectral data. At high magnetic fields, the elevated magnetic susceptibility effect results in an even shorter T_2^*. Consequently, the natural linewidth of metabolites increases. To create a homogeneous magnetic field over the VOI for spectroscopy, several methods have been proposed to improve field homogeneity by adjusting the corresponding coils (shim coils), which are controlled by passing electric currents to create gradients of various shapes. Before applying any adjustments, mapping the magnetic field distribution is necessary, using a 3D gradient echo mapping or a series of 2D projection (Gruetter, 1993; Gruetter and Tkáč, 2000).

The first- and second-order shims available for both experimental and many clinical magnet settings typically are sufficient to obtain satisfactory field homogeneity over the VOI, including those in mouse brain where magnetic susceptibility artifacts are amplified at high magnetic fields (Lei et al., 2010b; Tkác et al., 2004, 2007). Therefore, automatic adjustments of these shim terms or even higher-order shim terms (Gruetter, 1993; Gruetter and Boesch, 1992; Gruetter and Tkáč, 2000; Hetherington et al., 2006; Miyasaka et al., 2006; Schneider and Glover, 1991; Shen et al., 1999; Zhang et al., 2009) are necessary for studying the most common VOI in the rodent brain.

In vivo ^{1}H NMR spectroscopy of the brain

Methods for ^{1}H MRS localization

The full chemical shift range of most biologically interesting proton resonances is approximately within a range of 4 ppm, which must be excited and acquired. In addition, endogenous water occupies nearly 80% of brain tissue. Thus, the water signal is several orders of magnitude stronger than that of metabolites. In addition, signals from extra-cerebral tissue, i.e. subcutaneous lipid can cause artifacts and thus obscure cerebral signals. Therefore, adequate localization of ^{1}H signals is a prerequisite to acquire metabolites from the target VOI with minimal non-cerebral and water signals.

In the following, we provide a brief account of some techniques used for ^{1}H MRS of brain.

Image Selected In vivo Spectroscopy (ISIS)

Ordidge et al. (1986) described a full 3D localization with eight scans, including a non-selective excitation and three frequency slice-selective inversion pulses applied in the presence of three orthogonal gradients. For 1D ISIS, two scans, with and without one spatial selective inversion pulse are required to localize this particular slice. Due to the immediate acquisition of signal after excitation, ISIS can be used to acquire metabolites with relatively short T_2.

$$[\mathrm{ISIS}\text{-}90^\circ\text{-}\mathrm{acquisition}] \times 8$$

In order to achieve a 3D volume localization, 8 scans must be acquired with proper combination of slice-selective inversion pulses on or off. Therefore, ISIS remains sensitive to subtraction errors due to motion. When using a surface coil to achieve higher sensitivity, this subtraction error can be reduced, whereas effects of B_1 inhomogeneity can be minimized by using adiabatic pulses for selective inversion (AFP) and excitation (adiabatic-half-passage (AHP) or BIR-4(Garwood and Ke, 1991) pulses).

Point Resolved Spectroscopy (PRESS)

PRESS is based on a slice selective excitation, which is followed by two frequency selective-refocusing pulses, a so-called double spin echo method (Bottomly, 1984, 1987). Immediately after 90° and the first 180° pulses, the first echo contains signals from an intersection of two orthogonal slices defined by these two slice-selective pulses. With applying the second 180° pulse, the second spin echo contains only signals from the defined 3D volume. With such scheme, the signals outside the VOI are either not excited or defocused (spoiled).

$$90^\circ\text{-}t_1\text{-}180^\circ\text{-}t_1 + t_2\text{-}180^\circ\text{-}t_2\text{-}\mathrm{acquisition},$$

where

$$2 * t1 + 2 * t2 = \mathrm{TE}.$$

Adiabatic refocusing pulses have good slice profiles but they must be used in pairs. A pair of hyperbolic secant type pulses can provide better slice profile than a classical (e.g. sinc-shaped) refocusing pulse, however, they increase echo time (see also the LASER technique below).

Stimulated Echo Acquisition Mode (STEAM) spectroscopy

STEAM allows localizing the VOI with one single acquisition. This technique is based on Hahn echoes (Hahn, 1950) by using three 90° frequency selective RF pulses in the presence of magnetic field gradients.

$$90^\circ - \mathrm{TE}/2 - 90^\circ - \mathrm{TM} - 90^\circ - \mathrm{TE}/2 - \mathrm{acquisition}$$

The method requires either crusher gradients in the TM period and in both TE/2 periods to eliminate unwanted spin echoes and FIDs. Along with the improved gradient performance and asymmetric RF pulses, ^{1}H MRS can be obtained at a 1 ms echo time (Tkáč et al., 1999). However, compared to PRESS, half of signal is lost since the second RF pulse only rotates half of the magnetization while the other half is dephased by the crusher gradients.

Outer volume saturation (OVS) is widely used to eliminate unwanted but incompletely suppressed signals such as the strong extra-cerebral lipid signals from outside of the VOI, particularly in ultra-short echo time spectroscopy when asymmetric pulses were applied (Mlynárik et al., 2006; Tkáč et al., 1999). This is because that despite only about 25% of the asymmetric RF pulse duration time

contributes to the echo time period and greatly reduced rephasing gradients, frequencies outside the nominal bandwidth of these asymmetric pulses do not tend to cancel out as those from sinc pulses (Tkáč et al., 1999). The localized ^{1}H MRS methods using asymmetric pulses did present contaminations from outside the VOI (Boer et al., 2011; Oz and Tkáč, 2011), which can be eliminated with the optimized OVS (Mlynárik et al., 2006; Tkáč et al., 1999; Oz and Tkáč, 2011).

Localization by Adiabatic Selective Refocusing (LASER) spectroscopy

A single-scan 3D localization uses adiabatic excitation and refocusing RF pulses (Garwood and DelaBarre, 2001). Three pairs of adiabatic-full-passage (AFP) RF pulses are used for generating multiple spin echo and defining a 3D volume.

$$\mathrm{AHP\text{-}[AFP{-}AFP]\times 3\text{-}acquisition}$$

With an increasing magnetic field, increased spectral bandwidth requires intrinsically higher RF power to achieve the identical bandwidths, which will limit its application in MR measurements within SAR limits. Recently, an asymmetric slice-selective RF pulse has been used for frequency selective excitation. In consequence, the numbers of AFP pulses were reduced to two pairs, so called semi-LASER (Boer et al., 2011; Oz and Tkáč, 2011). This particular pulse sequence allows echo time to be shortened. Nevertheless, extra efforts, such as OVS and adjusting dephasing gradients are necessary for the elimination of signals from outside the VOI (also necessary for PRESS).

SPin ECho full Intensity Acquired Localized (SPECIAL) spectroscopy

The SPECIAL sequence is a combination of 1D ISIS in one direction followed by a slice-selective spin-echo in the other two orthogonal orientations (Mlynárik et al., 2006).

$$\mathrm{1D{-}ISIS_Y\text{-}90^\circ\text{-}180^\circ\text{-}acquisition}$$

In combination with the adiabatic 180° slice selection (in ISIS), this sequence employs two additional asymmetric pulses to achieve a final 3D definition with the echo time (Boer et al., 2011; Mekle et al., 2009; Mlynárik et al., 2006) similar to that in STEAM (Tkáč et al., 1999).

Since a 1D ISIS component is included for localization scheme, at least two scans are required for localization of the third dimension, which makes this sequence sensitive to motion. However, in combination with efficient OVS, a substantial number of studies in human and rodent brains showed similar spectral quality as that of STEAM at short echo time but with doubled sensitivity (e.g. Duarte et al., 2009a; Kulak et al., 2010; Lei et al., 2009, 2010a,b; Mekle et al., 2009; Mlynárik et al., 2006, 2008a).

Short echo time localization pulse sequences are desirable to maximize the information in the ^{1}H NMR spectra (Pfeuffer et al., 1999). The use of short TE allows to minimize J-modulation of coupled spin systems, which form the majority of MR detectable cerebral metabolites, and to reduce signal losses caused by T_2 relaxation. T_2 relaxation times are significantly shorter at high magnetic fields (Xin et al., 2008) and are difficult to quantify for coupled spin systems *in vivo*. In addition, a long repetition time (TR) allows eliminating effects of unknown T_1 relaxation times.

Water suppression

Water occupies approximately 80% of the total weight of brain tissue and represents the most abundant signal in proton MRS at ~4.7 ppm. This leads among others to a distorted baseline and spurious signals, which in turn make the detection of metabolites unreliable. Therefore, elimination of water signal improves the reliability of *in vivo* spectra quantification.

In general, suppression of a particular resonance in NMR requires a difference in a property between compounds of interest and the interfering compound. Several suppression methods are available, such as frequency selective and/or defocusing, exploiting different relaxation properties, spectral editing and others. Since water has a unique chemical shift apart from most metabolites, water suppression for short echo time ^{1}H MRS mostly relies on frequency-selective pulses. Seven such pulses (VAPOR) with optimal flip angle and timing allows for efficient water suppression in *in vivo* brain studies (Mlynárik et al., 2006; Tkáč et al., 1999; Oz and Tkáč, 2011), in spite of variations in the RF field amplitude and T_1 of water.

Chemical shift displacement error

All localization methods described above are based on applying a RF pulse in the presence of a gradient. For this reason, with frequency difference ($\Delta\omega$), localization is shifted by $\Delta x = \frac{\Delta\omega}{\gamma G_x}$, where G_x is the

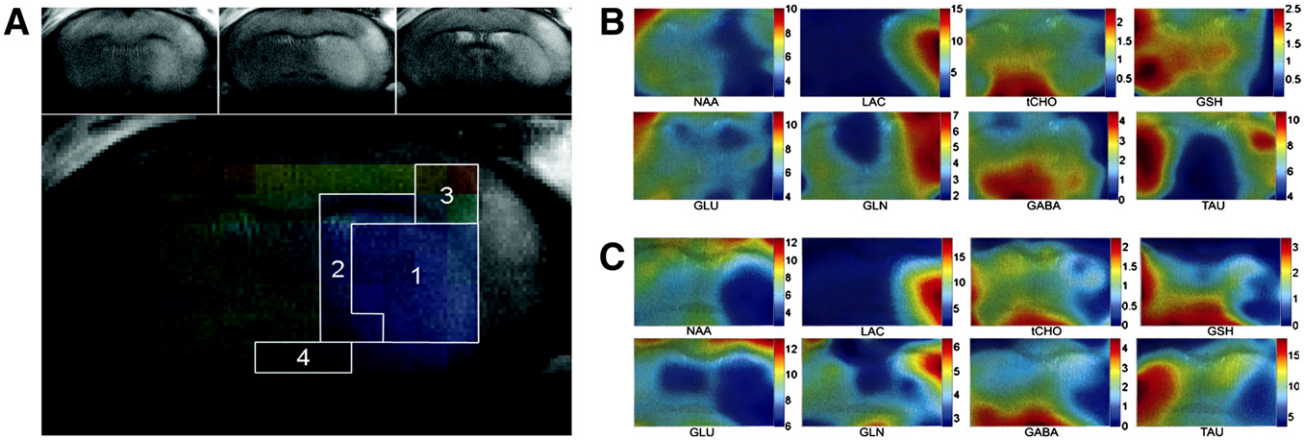

Fig. 2. Spectroscopic imaging of the mouse brain after focal ischemia provides high-resolution spatial mapping of neurochemical changes. Panel A depicts the position of the volume for spectroscopic imaging acquisition. Upper row: T2-weighted coronal images at 24 h after transient ischemia contributing to the spectroscopic imaging signal. Intensity changes can be seen in the affected region on the right hemisphere. Bottom: Overlay of the corresponding NAA map and indication of the ischemic core [1], penumbra [2], cortical penumbra [3] and hypothalamus [4]. Panels B and C show metabolite maps overlayed on the corresponding anatomical images after 3 h (B) and 24 h (C), color scale in μmol/g. The maps represent the VOI as shown in panel A. Typical spatial patterns can be observed in the contralateral hemisphere, *i.e.* on the left hand side, such as high cortical glutamate and high striatal taurine, also GABA concentration is high in the hypothalamus.
Figure was reproduced from Alf et al., 2011 with authorization of the publisher.

slice-selective gradient strength and γ is the gyromagnetic ratio. This effect is called chemical shift displacement error. For example, given $G_x = 400$ mT/m and 5 ppm chemical shift range for proton ($\gamma = 42$ MHz/T) at 400 MHz, the maximum displacement errors, 2.5 ppm away from the transmitter offset, are not more than 0.06 mm. With increased field strengths, spectral dispersion increases and so does the chemical shift displacement error.

Spectroscopic imaging

On the other hand, while the localization techniques described above allow signal detection from a well-defined volume, spectroscopic imaging, also called chemical shift imaging (CSI), allows the detection of multiple spectra (e.g. Brown et al., 1982). However, these multivoxel NMR spectroscopy methods are intrinsically affected by inhomogeneity across the large measured volume and require long data acquisition times. Nonetheless, spectroscopic imaging can be performed in rodents with μL spatial resolution, which is comparable to other imaging modalities, for example animal positron emission tomography (PET). A neurochemical profile of more than 10 metabolites at short echo-time in the rat brain has thus been imaged at 9.4 T (Mlynárik et al., 2006, 2008b; Weiss et al., 2009).

Spectroscopic imaging is particularly useful in the diagnosis of ischemic injuries (Fig. 2), being capable to identify the neurochemical profile in the infarct region, edematous tissue, penumbra and healthy unlesioned tissue (e.g. Alf et al., 2011; Cvoro et al., 2009; Mlynárik et al., 2008a). Similarly, the study of cerebral tumors benefits from the possibility of detecting different metabolic states (edema, necrosis, neoplastic cells) in the lesion (e.g. Löbel et al., 2011; Server et al., 2010; Simões et al., 2010).

Table 1
Neurochemical profile detected in the cerebral cortex of adult C57BL/6 mice at 14.1 T (from Kulak et al., 2010; Duarte et al., 2011), Sprague–Dawley rats at 9.4 T (from Lei et al., 2009; Xin et al., 2010a) and humans at 3.0, 7.0 T (from Gambarota et al., 2009; Mekle et al., 2009) and at 9.4 T (Deelchand et al., 2010).

	Mouse cortex	Rat cortex	Human occipital cortex
Alanine	0.9–1.2	0.4–0.6	0.3[a]
Aspartate	1.8–2.3	1.9–2.6	2.1–3.1
Phosphorylcholine (PCho)	0.5–0.6	0.4–0.5	–
Creatine[b]	3.9–4.5	2.7–3.8	3.2–5.8
Phosphocreatine[b]	3.6–4.3	3.8–5.2	2.2–4.5
γ-aminobutyrate (GABA)	1.7–2.0	1.1–1.4	1.3–2.5
Glutamine	3.6–3.9	3.5–4.3	1.6–2.2
Glutamate	10.3–11.2	10.3–12.9	8.9–12.8
Glutathione	1.2–1.4	0.7–1.2	1.1–1.4
Glycine	0.9–1.5	0.6–0.9	1.2[c]
myo-inositol	4.4–4.8	3.8–4.5	4.9–5.7
Lactate[b]	1.6–2.1	0.4–1.6	0.5–0.7
N-acetylaspartate	8.7–9.7	8.6–10.5	11.0–13.5
scyllo-inositol	0.2[d]	0.1–0.2	0.3–0.4
Taurine	8.9–11.0	5.0–6.9	1.3–3.3
Ascorbate	1.2–2.1	1.0–1.6	1.4[d]
Glucose[b]	1.6–2.0	2.2–4.1	1.4–2.24
N-acetylaspartylglutamate (NAAG)	0.6–0.9	0.3–0.7	1.0–1.1
Glycerylphosphorylcholine (GPC)	0.5–0.8	0.1–0.2	–
Phosphorylethanolamine	1.7–1.9	1.8–2.1	1.6–2.8
β-hydroxybutyrate[b]	–	0.5–1.3	–
GPC + PCho[e]	1.0–1.2	0.5–0.8	0.9–1.1

[a] Only reported by Deelchand et al. (2010).
[b] Dependent on nutritional state and anesthesia.
[c] Only reported by Gambarota et al. (2009).
[d] Only reported by Kulak et al. (2010).
[e] Often the concentration of each choline metabolite is not reported and therefore total concentration of choline-containing metabolites is given.

Quantification of *in vivo* ^{1}H NMR spectra

The NMR signal acquired with localized ^{1}H MRS methods is, in principle, proportional to the induced transverse magnetization of spins originating from the targeting volume. Despite the sample itself, instrumental factors and an MR pulse sequence can influence the direct calculation of the corresponding metabolite concentration. By using validated reference methods, MRS signals can be quantified to provide biochemical information.

There are two main approaches for non-invasive quantification, i.e. internal and external reference methods. The internal referentiation is generally made by normalization of the signals to a known (assumed constant) concentration. Frequently, total creatine is used as a reference for the remaining metabolite concentrations. However, its concentration (signal) may change in pathological conditions (Duarte et al., 2009a,c, 2011), with age (Kulak et al., 2010) and between gray and white mater (Mukherjee et al., 2000). Therefore, most often a non-water-suppressed spectrum is acquired under the same experimental conditions. From the water content, concentration is calculated. Attention should be given to the fact that water content changes when pathologies lead to reduction of brain mass and ventricle enlargement or in the case of edema, and varies with age (e.g. Kulak et al., 2010; Tkáč et al., 2003 and references therein).

The external reference method applies the identical settings of an *in vivo* experiment on an *in vitro* solution containing metabolites of known concentrations. This method is suitable for metabolites having known or similar relativity properties between *in vivo* and *in vitro*, and presenting less complicated spectral patterns while high spectral resolution is offered, for example in ^{13}C MRS (e.g. see review Gruetter et al., 2003) and with spectral editing (Terpstra et al., 2002). The peak areas can be quantified by numerical integration for visible and prominent metabolite resonances.

The ^{1}H MR spectral pattern is complex and severely overlapped. Although with increased magnetic field strength these problems are reduced, signal overlap remains. Therefore, methods allowing

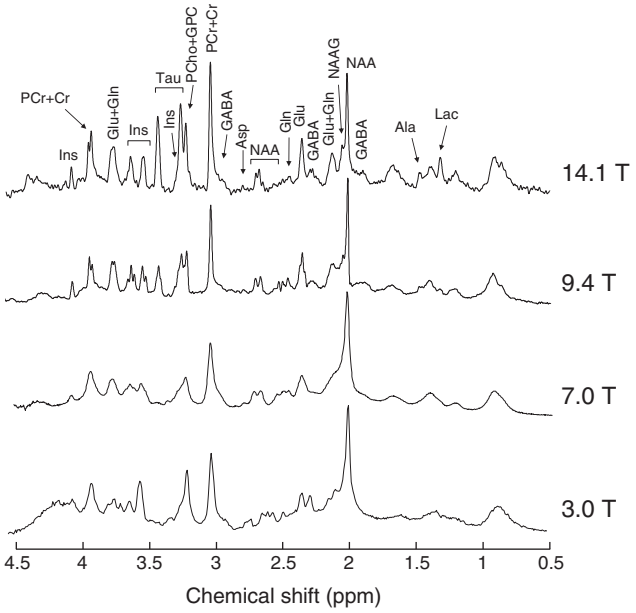

Fig. 3. Localized ^{1}H NMR spectra acquired with SPECIAL spectroscopy at different magnetic fields. Spectra at 3.0 and 7.0 T were acquired from cortical regions of the human. Spectra at 9.4 and 14.1 T are from the hippocampus of the rat and mouse, respectively. Metabolites in the spectra are assigned as follows: *myo*-inositol (Ins), phosphocreatine (PCr), creatine (Cr), glutamate (Glu), glutamine (Gln), taurine (Tau), glycerophosphorylcholine (GPC) phosphorylcholine (PCho), γ-aminobutyrate (GABA), aspartate (Asp), *N*-acetylaspartate (NAA), *N*-acetylaspartylglutamate (NAAG), alanine (Ala), lactate (Lac).

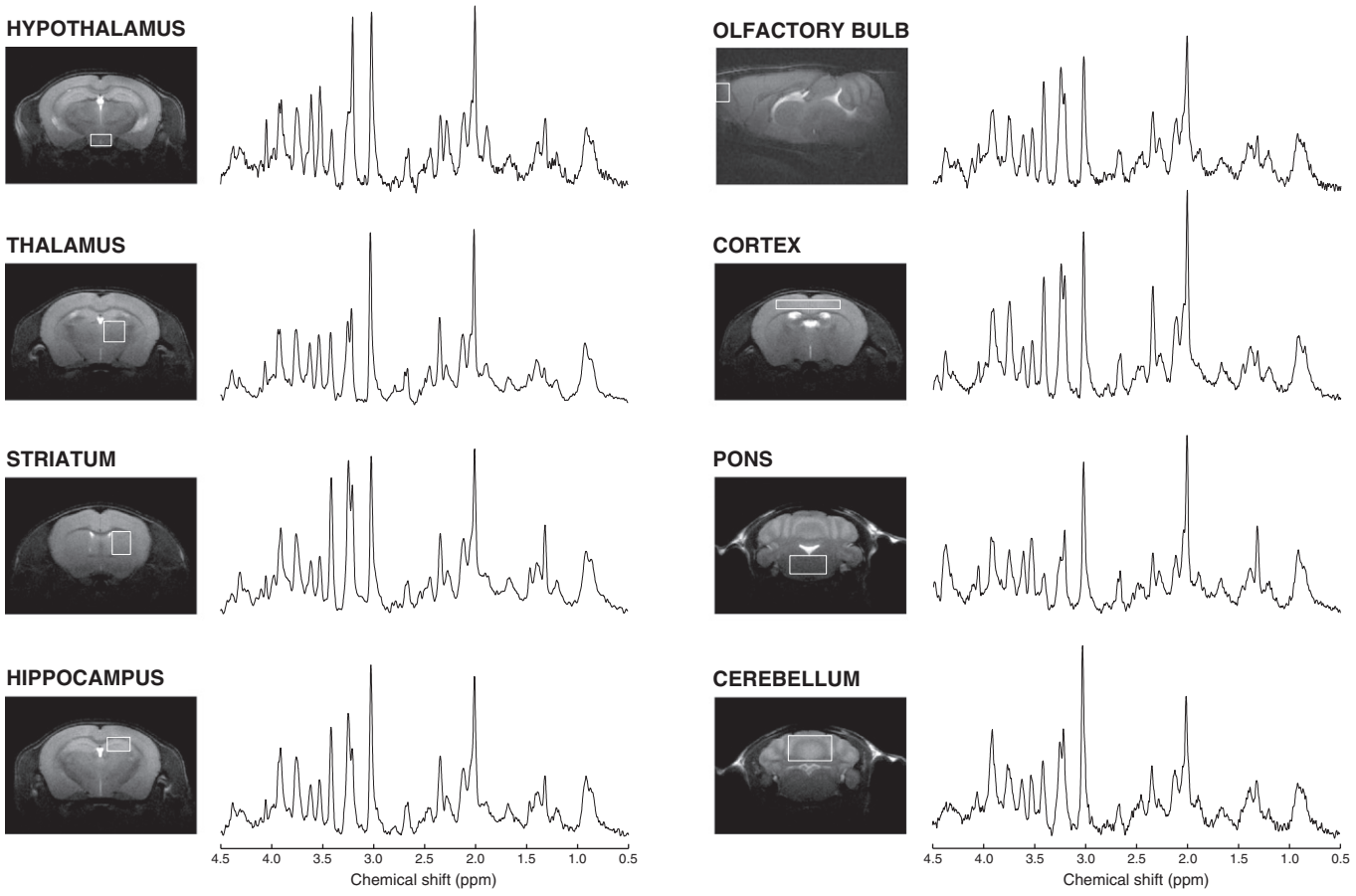

Fig. 4. Regional specificity of ^{1}H NMR spectroscopy of the brain. Spectra were acquired from the mouse brain at 14.1 T using SPECIAL.

analysis of such spectra require advanced fitting algorithms. There are several approaches available that use prior knowledge, such as VARPRO, AMARES, LCModel and others (Abildgaard et al., 1988; de Graaf and Bovee, 1990; Naressi et al., 2001; Provencher, 1993; Slotboom et al., 1998; Van der Veen et al., 1988; Vanhamme et al., 1997). For ^{1}H MRS, LCModel adjusts the amplitudes, line widths and phases of the metabolite basis set to match the *in vivo* and *in vitro* spectra as close as possible (de Graaf et al., 2011; Pfeuffer et al., 1999; Provencher, 1993).

The neurochemical profile detected by ^{1}H NMR spectroscopy

Metabolite concentrations often reflect the activity of metabolic processes. At high magnetic field, nowadays considered 7 T and above, a neurochemical profile of more than 20 metabolites can be determined in a non-invasive way under normal physiological conditions (Fig. 1). As general rule, ^{1}H NMR spectroscopy can detect all compounds existing in a concentration above 0.5 μmol/g.

The concentrations of most brain metabolites within the neurochemical profile are modified during development reflecting the structural and functional evolution inherent to the differentiation of cerebral networks (e.g. Kulak et al., 2010; Tkáč et al., 2003). The neurochemical profile is region specific (Kulak et al., 2010; Lei et al., 2010b; Tkáč et al., 2003, 2004; Xin et al., 2010a), reflects functional states (Mangia et al., 2007) and is affected by pathological conditions (e.g. Duarte et al., 2009a, 2011; Lei et al., 2009; Tkáč et al., 2007; van de Looij et al., 2011a,b). Therefore, the non-invasively detected neurochemical profile may be taken as a marker for specific metabolic states that are associated with degeneration or acute injury as is discussed in the present review. In addition, for a given brain area, the neurochemical profile is species dependent (see Table 1) and it may even vary within different strains of the same species (Tkáč et al., 2004). As such, although brain metabolism has wide differences among species namely when comparing rodents to humans, once the role of the measured neurochemicals is understood, high resolution NMR qualifies as method of choice for *in vivo* translational investigations of preclinical animal models of human neurological and psychiatric pathologies during development or aging.

For example, the metabolites composing the neurochemical profile detected by non-invasive ^{1}H NMR spectroscopy in the adult cortex are depicted in Table 1, for mice, rats and humans. Spectral quality from 3 to 14.1 T and regional differences in spectral paters can be appreciated in Figs. 3 and 4, respectively.

Neurotransmitter metabolism

Amino acid neurotransmitters are the most abundant transmitters in the central nervous system playing an important role in the wiring of neuronal networks and organizing cyto-architecture during cerebral development and differentiation. Their concentrations are strongly altered if the neuronal network is disrupted upon injury. Glutamate and aspartate are the dominant excitatory amino acids. The concentrations of both increase steadily during early development until adulthood, as measured *in vivo* in rats (Tkáč et al., 2003) and mice (Kulak et al., 2010). The fast early concentration rise especially of glutamate closely parallels the time course of glutamatergic synaptogenesis and marks a period of ongoing refinement of the cerebral circuitry. As glutamatergic synapses develop and mature, energy demand rises. Thus, this early period is also associated with a major step in the maturation of energy metabolism, demonstrated by the concomitant modification in the brain levels of glucose and lactate (discussed below).

Glutamate and aspartate are further involved in the transference of reducing equivalents produced in the glycolysis from the cytosol into the mitochondrial matrix through the malate–aspartate shuttle, a major step in neuroenergetics (Gruetter et al., 2003; McKenna, 2007). Therefore, these two amino acids are used in processes that may link excitatory neurotransmission to energy production and usage.

Glutamine is synthesized from glutamate by glutamine synthetase in glia and converted back to glutamate by glutaminase in neurons, completing the glutamate–glutamine cycle. This cycle is not stoichiometric (McKenna, 2007) and both glutamate and glutamine are engaged in a number of important metabolic pathways like energy provision, synthesis of important chemicals like *N*-acetylaspartate (NAA), *N*-acetylaspartylglutamate (NAAG), γ-aminobutyrate (GABA) and glutathione (GSH), and protein synthesis. Thus, it is expected that glutamate and glutamine concentrations develop similarly as both are functionally coupled through this glutamate–glutamine cycle (for review see e.g. Zwingmann and Butterworth, 2005).

Glutamine is synthesized and mainly present in the glia. Its concentrations rise within the first weeks of life in the rat (Tkáč et al., 2003) and mouse (Kulak et al., 2010) brain, similarly to those of glutamate, reflecting the maturation of the glio-vascular unit that supports neuronal function. Glutamine synthesis is also used for ammonia detoxification (Cudalbu et al., 2011) and has been shown to be a good marker of hepatic encephalopathy (Behar et al., 1999; Córdoba et al., 2002; Kreis et al., 1991).

For a long time, non-invasive detection of a peak corresponding mainly to resonances of glutamate and glutamine in cerebral tissue has been taken as a marker of function and degeneration in preclinical and clinical studies. Only the advances of the last decade and the increase in magnetic field strength allowed independent quantification of both glutamate and glutamine. An independent measure of both and also their ratio may be a better marker to indicate neuronal function, as glutamate and glutamine are mostly located in neurons and glia, respectively. For example, impaired neurotransmission and excitotoxicity after an ischemic insult lead to transient glutamate decrease and glutamine accumulation (Berthet et al., 2011; Lei et al., 2009). In line with this idea, disturbed glutamatergic neurotransmission in anterior regions of the schizophrenic brain leads to altered levels of glutamine, glutamate and most notably of glutamine to glutamate ratio, as observed in clinical ^{1}H NMR spectroscopy studies (Bustillo et al., 2009; Lutkenhoff et al., 2008; Shirayama et al., 2010; Tayoshi et al., 2009).

Glutamate can be decarboxylated to GABA for use in GABAergic neurotransmission. A significant pool of brain glutamate is involved in this process (discussed in Hertz, 2006). Although GABA concentrations remain stable throughout development (Kulak et al., 2010; Tkáč et al., 2003), modifications in metabolic and signaling fates of GABA occur at the time of GABAergic inhibitory synapse formation (Anderson et al., 1995) and with the increment of cortical GABA binding sites (Skerritt and Johnston, 1982). At low magnetic fields, GABA is difficult to measure in ^{1}H NMR spectra and its detection has been achieved by editing techniques, which are not exempt of quantification errors (Bielicki et al., 2004; Choi et al., 2005; Mescher et al., 1998; Terpstra et al., 2002). Higher magnetic fields, on the other hand, provide increased spectral resolution making GABA quantifiable (Deelchand et al., 2010; Gambarota et al., 2009; Mekle et al., 2009; Oz et al., 2006). GABA concentrations were found to be affected by neurological disorders like epilepsy (Doelken et al., 2010; Goddard et al., 2001; Simister et al., 2003), schizophrenia (Yoon et al., 2010), depression (Sanacora et al., 2004) or substance abuse (Behar et al., 1999; Ke et al., 2004).

NAAG is a highly abundant neuromodulatory peptide in the brain that is expressed in neuronal terminals (Shave et al., 2001) and to lesser extent in glial cells (Cassidy and Neale, 1993). It is synthesized from NAA under tight regulation and acts on presynaptic metabotropic glutamate receptors mGluR2/3 to down-regulate neurotransmitter release via negative feedback (Zhao et al., 2001) and on *N*-methyl-D-aspartate (NMDA) receptors either as direct agonist (e.g. Westbrook et al., 1986) or antagonist (e.g. Burlina et al., 1994). NAAG levels detected *in vivo* in the mouse brain are highest after birth and decline thereafter to reach a stable plateau at adult age (Kulak et al., 2010). This exactly mimics early results obtained with tissue extracts (Koller and Coyle, 1984).

Glycine has a dual role as inhibitory neurotransmitter, on one hand activating glycine receptors, and on the other as co-agonist for glutamate excitatory transmission through NMDA receptors (Betz and Laube, 2006). The proton resonances of glycine are a singlet overlapping with a more intense resonance of myo-inositol. This singlet was detected in the brain of both rodents (Gambarota et al., 2008; Xin et al., 2010a) and humans (Gambarota et al., 2009). Glycine is particularly highly concentrated in the brain stem, namely in medulla oblongata (Xin et al., 2010a), where a large portion of synapses are involved in glycinergic neurotransmission. Like for NAAG, the highest glycine concentrations in the brain are observed at P10 and decline until adulthood (Kulak et al., 2010). In fact, the rate of glycine synthesis peaks around 10–15 days after birth (Benítez-Diaz et al., 2003; Lahoya et al., 1980) and likewise, during this period, glycine receptors undergo a major switch of the relative expression of glycinergic subunits (Lynch, 2004). It is interesting to note that the increase in levels of excitatory neurotransmitters, glutamate and aspartate (NMDA receptor agonists), is paralleled by a reduction in the concentration of its modulator NAAG as well as its co-agonist glycine.

Taurine is, among other functions, also a neuromodulator (Gupta et al., 2009). Taurine released from neurons and glia interacts with inhibitory $GABA_A$, $GABA_B$ or glycine receptors (reviewed in Albrecht and Schousboe, 2005) thus displaying capability of modulating synaptic plasticity (e.g. del Olmo et al., 2000). This inhibitory role of taurine is especially important during the period of cortical synaptogenesis (Flint et al., 1998), when brain taurine levels are found to be highest (Kulak et al., 2010; Tkáč et al., 2003). Like glycine and NAAG, taurine concentration in the brain decreased during development to adult age (Kulak et al., 2010; Tkáč et al., 2003). However, as a small fraction of taurine is involved in neuromodulation (particularly in the case of rodents), the main role of taurine may be rather related to osmoregulation, balancing the increase in glutamate, glutamine, NAA and other neurochemicals during development (Kulak et al., 2010) and counteracting osmolarity imbalance upon brain injury (Berthet et al., 2011; Lei et al., 2009). Interestingly, taurine concentrations in the human brain are relatively low (Table 1) and the role in neuromodulation may be more important than in controlling cell volume and osmolarity.

Cellular proliferation and membrane lipid metabolism

N-acetylaspartate (NAA) is among the most abundant neurochemicals, with concentrations on the order of 10 μmol/g in the human and rodent brain (Table 1). NAA is generally taken as a putative neuronal marker with its almost exclusive localization in neurons, turning it in a reliable diagnostic marker. In fact, NAA levels are frequently found to be absent in tumors of glial origin (e.g. Sibtain et al., 2007) and to decrease in neuropathological conditions, correlating with the degree of degeneration in humans (Bruhn et al., 1989; Gideon et al., 1992, 1994; Horská et al., 2009; Kantarci, 2007) and rodents (e.g. Berthet et al., 2011; Lei et al., 2009; Tkáč et al., 2007). In addition, after transient ischemia and brain injury without neuronal death, NAA levels are able to recover (Brulatout et al., 1996; De Stefano et al., 1995), suggesting it as a marker of neuronal functionality rather than neuronal density.

Developmental increase of NAA content in cortical regions of the rodent (Kulak et al., 2010; Tkáč et al., 2003) or human brain (Ross and Blüml, 2001) may be associated with neuronal proliferation and its role in lipid and myelin synthesis (Burri et al., 1991; D'Adamo and Yatsu, 1966). Accordingly, axonal demyelination is associated with reduction of NAA (Bitsch et al., 1999). Although NAA is mainly synthesized and stored in neurons from mitochondrial acetyl-CoA and aspartate (Baslow, 2003), its deacetylation occurs in

oligodendrocytes (Kirmani et al., 2002). In oligodendrocytes, NAA can replenish both acetyl-CoA and oxaloacetate (through aspartate) pools providing carbon skeletons for both energy production and local lipid synthesis, required in the myelination process. The significant reduction in PE and increase in NAA concentrations in the cerebral cortex from P20 onwards may reflect the rate of deposition of myelin that is very rapid between P14 and P30 yet continues afterwards at slower rate (Costantino-Ceccarini and Morell, 1972; Muse et al., 2001). In line with this role of NAA, Canavans disease is characterized by accumulation of NAA due to impaired deacetylation in olygodendrocytes, which is associated to defects in myelin synthesis and deposition (Chakraborty et al., 2001).

Inositol has several isomers, being *myo*-inositol (~4 μmol/g) the main contributor to the peak observed in ^{1}H NMR spectra of the brain. The second most concentrated isomer is *scyllo*-inositol (~0.2 μmol/g) that possesses six symmetric protons and originates a singlet at 3.34 ppm. The increase of *myo*-inositol concentration during development (Kulak et al., 2010; Tkáč et al., 2003) seems to be related to the demand for synthesis of inositol-containing phospholipids during synaptogenesis, axonal growth and myelination. Accordingly, Yao et al. (1999) reported an increase of phosphatidylinositol that may be incorporated into lipid membranes (Quarles et al., 2006) during mouse brain development. In several neurological disorders, *myo*-inositol was found to be increased (Bitsch et al., 1999; Horská et al., 2009; Kantarci, 2007) and this is generally assumed to be a marker of gliosis, based on the fact that higher *myo*-inositol levels are found in cultured astrocytes as compared to neurons *in vitro* (Brand et al., 1993; Glanville et al., 1989). However, brain *myo*-inositol levels may not always correlate with other molecular markers of gliosis (Duarte et al., 2009a; Kim et al., 2005; Kunz et al., 2011).

Choline-containing compounds are essential for membrane lipid synthesis and act as precursors for the biosynthesis of the neurotransmitter acetylcholine. The methyl protons of choline-containing compounds all resonate at 3.2 ppm. In the brain, choline is below the NMR detection limit and mainly glycerylphosphorylcholine (GPC) and phosphorylcholine (PCho) contribute to this intense resonance (e.g. Klein, 2000). At a high magnetic field, namely 14.1 T, it was possible to quantify the two phosphorylated compounds of choline through the distinct multiplicity of their remaining resonances (Kulak et al., 2010; Mlynárik et al., 2006).

Choline availability seems crucial for the onset of GABAergic neuronal differentiation, especially during embryonic brain development (Albright et al., 2003) and progenitor cell proliferation and apoptosis in mouse brain (Craciunescu et al., 2003). Modification of cerebral choline concentration during development was found to be region and species specific. In general, brain choline increases with age in the mouse brain (Kulak et al., 2010) but not in rats (Tkáč et al., 2003). In humans, using ^{31}P NMR spectroscopy, it was found that both phosphorylcholine and phosphorylethanolamine decrease during development with concomitant increase in the glycerylated forms of these phospholipids (Blüml et al., 1999).

Total choline concentration (including free choline and phosphorylated choline metabolites) in the human brain is positively correlated with age (e.g. Angelie et al., 2001; Chang et al., 1996; Kreis et al., 1993; Pfefferbaum et al., 1999a,b). This age-associated increase in choline has been attributed to increased release of water-soluble choline-containing compounds from cell membranes, reflecting higher membrane turnover (Chang et al., 1996). In line with this, choline-containing compounds are associated with high cellular proliferation and inflammatory responses in tumor growth and, therefore, choline is often taken as a marker for diagnosis of certain brain tumors (e.g. Kinoshita and Yokota, 1997; Li et al., 2007; Sibtain et al., 2007).

Phosphorylethanolamine (PE) is a precursor for phosphatidylethanolamine, which is a major phospholipid in the brain (Quarles et al., 2006). Phosphorylethanolamine concentration decreases during cerebral development and this observation is consistent in rodents and humans, paralleling the progression of myelination and cellular proliferation (Blüml et al., 1999; Gyulai et al., 1984; Kulak et al., 2010; Tkáč et al., 2003; Turner et al., 1994; Rao et al., 2003; Wijnen et al., 2010a). Like choline, increased PE metabolism during high cellular proliferation was found in several types of brain tumors and to correlate with tumor malignancy (e.g. Kinoshita and Yokota, 1997).

In general, for both rodents and humans, NAA concentration rises during development while choline and ethanolamine are reduced (Kulak et al., 2010; Ross and Bluml, 2001; Tkáč et al., 2003; Blüml et al., 1999). In the human brain, the concentration of NAA was found to be reduced upon aging (Chang et al., 1996; Gruber et al., 2008; Schuff et al., 1999, 2001), while choline and *myo*-inositol increased (Chang et al., 1996; Gruber et al., 2008). This suggests that cell membrane constitution and turnover are modified during development and aging, as is plasticity of neuronal circuits.

Energy metabolism

Depending on its physiological state and maturity, the brain utilizes different energy substrates including glucose, ketone bodies and lactate (e.g. Lust et al., 2003; Nehlig, 2004; Vannucci et al., 1994). In the brain of suckling rodents, ketone bodies can represent up to 70% of the total energy substrate pool (Nehlig, 2004). Rheims et al. (2009) have shown that, during early postnatal development, ketone body availability modulates GABA signaling and efficiently controls the excitability of neonatal cortical neurons.

In the mouse brain, lactate concentrations were found to be relatively unaltered during early development and increase at adult age (Kulak et al., 2010). In developing rats, Tkáč et al. (2003) did not observe changes in lactate concentration during cortical development, whereas Lust et al. (2003) found high lactate in neonate rats and a strong decrease in adults. Lactate generated and released by astrocytes has been suggested to serve as an energy substrate for neurons, especially during synaptic activity (Pellerin and Magistretti, 1994) and during re-oxygenation after stroke (Berthet et al., 2009). Ascorbate may play a role in this process by regulating glucose transport and glycolysis (Castro et al., 2009). Cerebral ascorbate concentration decreases during development to adult age (Kulak et al., 2010; Terpstra et al., 2010) therefore suggesting that ascorbate-induced glucose transport inhibition and lactate transport stimulation may be higher in early developmental stages than in adulthood. This corroborates the preferential use of other substrates rather than glucose by the developing brain (Lust et al., 2003).

Alanine is an amino acid with close links to metabolic pathways such as glycolysis, tricarboxylic acid cycle and protein synthesis. Like for lactate, with which it is in equilibrium though pyruvate, conflicting observations were reported for alanine concentrations in the developing rat brain (Bayer and McMurray, 1967; Burri et al., 1990; Tkáč et al., 2003). However, both *in vivo* and *in vitro* studies in mice demonstrated that cerebral alanine content is higher at birth and decreases during development (Kulak et al., 2010; Yao et al., 1999), reflecting the high protein turnover in the developing brain as result of cell proliferation and tissue expansion.

These events require availability of energy, typified in the larger concentration of phosphocreatine relative to creatine at early developmental ages. Total creatine content was found to increase in the cortex during development (Kulak et al., 2010), following the modification in brain creatine kinase activity (Manos et al., 1991), which is a critical component in maintaining brain energy homeostasis by buffering cellular energy demands.

More than buffering energy requirements, the creatine–phosphocreatine equilibrium is thought to be a mechanism for energy transport from the mitochondrial producing site to the synaptic consumption at the nerve terminals. Total creatine is more concentrated in gray than white matter (e.g. Pouwels and Frahm, 1998), and thus

can be thought as a putative neuronal marker. The total concentration of creatine is often assumed to be constant but is frequently found to be altered by acute brain injury and neurological disorders.

Other metabolites related to energy metabolism are often included in the neurochemical profile but not observable in normal subjects by *in vivo* ^{1}H NMR spectroscopy. Acetate is taken up by the brain and metabolized in glial cells (Cerdan et al., 1990; Waniewski and Martin, 1998) and is often used as tracer to probe astrocytic intermediary metabolism upon infusion in the blood stream (e.g. Xin et al., 2010b). Recently, Hong et al. (2011) claimed that the methyl protons of acetate can be detected in ^{1}H NMR spectra of the normal rat brain *in vivo* at 16.4 T. A large concentration of pyruvate, the end product of glycolysis, was detected *in vivo* in the brain of neonates with pyruvate dehydrogenase deficiency (Zand et al., 2003). Both acetate and pyruvate, which exist in undetectable concentrations, were detected at high levels in cystic lesions by *in vivo* ^{1}H NMR spectroscopy (Jayakumar et al., 2003; Kohli et al., 1995).

Metabolic disorders such as diabetes result in alterations of the neurochemical profile (Duarte et al., 2009a; Geissler et al., 2003; Kreis and Ross, 1992; van der Graaf et al., 2004), regarding metabolites involved in energy metabolism. Hyperglycemia increases brain levels of glucose and β-hydroxybutyrate, is an indicator of ketoacidosis, and is quantifiable at a high magnetic field (Duarte et al., 2009a; Lei et al., 2010a). Increased lactate concentrations are very common in certain acute insults or in brain disorders that affect mitochondrial function and upregulate the glycolytic pathway (e.g. Lei et al., 2009; van de Looij et al., 2011a).

Finally, it is very important to stress that the brain energy status depends on neuronal activity and, therefore, on the type and deepness of anesthesia used for the NMR study (Lei et al., 2010a). In addition, the nutritional conditions may also induce specific neurochemical patterns, especially when studying brain energy metabolism.

Osmoregulation

Osmolarity alterations trigger physiological responses that involve the balance of both ions (mainly sodium, potassium, and chloride) and organic compounds, i.e. idiogenic osmolytes, since in principle every metabolite occurring at high concentration is a potential regulator of cellular osmolarity. Osmolarity control in the brain is considered to occur mainly but not exclusively via the concentrations of taurine, creatine and *myo*-inositol. Hypoosmolarity induces their release while hyperosmolarity causes their slow accumulation (see Verbalis, 2010 for review). Taurine is known to have three main roles in the brain, namely acting as a neuromodulator (discussed above), an antioxidant and an osmoregulator (Albrecht and Schousboe, 2005; Gupta et al., 2009). Accordingly, its intracellular content changes in parallel with plasma osmolarity (Trachtman et al., 1992; Rose et al., 2000). Taurine is one of the most concentrated metabolites in the rodent brain, decreasing from about 20 mM at P10 to 10 mM in adult mice (Kulak et al., 2010; Weiss et al., 2009). Similar observations were reported in the rat (Tkáč et al., 2003). On the other hand, concentrations of *myo*-inositol and creatine increase during development of the rodent cortex (Kulak et al., 2010; Tkáč et al., 2003), balancing taurine reduction. Supporting their role in osmoregulation, for example, chronic hyponatremia leads to reduction of taurine, creatine, *myo*-inositol and also glutamate and glutamine (Verbalis, 2010). Chronic hyperglycemia alters osmolarity homeostasis and likewise the brain content of taurine, creatine and *myo*-inositol is increased (Duarte et al., 2009a; van der Graaf et al., 2004). NAA can be released to the interstitial space upon osmotic challenges (e.g. Sager et al., 1997; Bothwell et al., 2001) suggesting that it may also play a role in osmorelulation.

Antioxidant defense

Neurological disorders are often associated with deficiency of antioxidant protection systems (e.g. Ballatori et al., 2009; Do et al., 2009; Martin and Teismann, 2009). However, antioxidant compounds generally exist in low concentration and non-invasive detection is therefore challenging. Glutathione and ascorbate (vitamin C) are two major antioxidants that can be detected by ^{1}H NMR spectroscopy using e.g. selective editing techniques (e.g. An et al., 2009; Kaiser et al., 2010; Terpstra and Gruetter, 2004; Terpstra et al., 2003). At a high field, with gain in sensitivity and spectral resolution, direct detection of glutathione and ascorbate at short echo time is possible (e.g. Terpstra et al., 2005, 2006).

While ascorbate is predominantly in the neuronal compartment (Rice, 2000), glutathione is more concentrated in glia than neurons (Dringen, 2000), both existing under tight homeostatic regulation by synthesis and/or transport through the blood–brain-barrier. Glutathione acts in concert with ascorbate that is also an enzyme co-factor in the brain and is involved in maintenance of brain homeosthasis. As such, ascorbate is involved in antioxidant protection and regulation of glucose metabolism (Castro et al., 2009), but not exclusively. It also plays a role in myelin formation (Eldridge et al., 1987), enhancement of synaptic activity (Rebec and Pierce, 1994) and direct protection from excitotoxicity (Qiu et al., 2007). *In vivo* ^{1}H NMR spectroscopy revealed high ascorbate concentrations in young (P10) animals and a subsequent steady decline until adulthood (Kulak et al., 2010; Terpstra et al., 2010), while glutathione remains approximately constant (Kulak et al., 2010; Tkáč et al., 2003). In line with this are observations that young rodents are more prone to oxidative stress than are mature animals (Lykkesfeldt, 2002) and that the developing rodent brain is particularly susceptible to vitamin C deficiency because of rapid cellular growth and immature antioxidant defense systems (Lykkesfeldt et al., 2007). Indeed, ascorbate deficiency in early postnatal life results in impaired neuronal development and spatial memory deficits (Tveden-Nyborg et al., 2009), which are associated with brain areas that normally contain higher levels of ascorbate, namely the hippocampus and cortex (Rice, 2000).

Rodents such as mice and rats, in contrast to humans, are able to endogenously synthesize ascorbate and can adapt its synthesis according to demand (Rice, 2000). As the organism and its antioxidant systems mature, less ascorbate is needed and synthesis is down-regulated (Kulak et al., 2010).

Translational research from animal models to clinical applications

The discovery of sensitive biomarkers that indicate disease progression is useful for identification of beneficial treatments. A biomarker ideally is sensitive and specific for a particular disorder and manifests changes before irreversible structural alterations take place. Blood is the most convenient source of biomarkers for pathology assessment. This is however limited to the use in diagnosis of autoimmune, metabolic or genetic disorders that affect the CNS. In addition, neurodegeneration processes are in most cases not reflected in peripheral tissues as they affect only regions of the brain. MR methods are nowadays the best non-invasive tools to address cerebral status or function. However, similar metabolic alterations can occur in different neurological disorders and may lead to similar modifications in ^{1}H NMR spectra acquired *in vivo*. Thus, instead of determining each metabolite per se, the neurochemical profile mapped throughout the brain using e.g. spectroscopic imaging must be viewed as a whole biomarker consisting of not only the neurochemical concentrations but also the regional specificity associated to each CNS disorder.

As discussed above, brain NAA concentration increases during development to adulthood in rodents and humans and reduces upon progression of neurodegeneration. With NAA, also myo-inositol may be modified upon neuronal injury and degeneration, being usually assumed to be a marker of gliosis. Therefore, these are examples of easily detectable metabolites at low magnetic fields and often taken as markers for tissue differentiation or progression of neurological

disorders. In addition, mitochondria are central regulators of neuronal homeostasis and cell survival, and increasingly viewed as central players in several aging-related neurodegenerative diseases (Lin and Beal, 2006). Consequently, evaluation of neurochemicals that are directly related to bioenergetics is important in neurodegeneration. For these, however, quantification requires use of higher magnetic fields.

Most MR scanners available for clinical routine are operating at a low magnetic field. Therefore the extensive neurochemical profile observed in animal studies is not directly applicable to the clinical environment. Nevertheless, even at 1.5 T, several metabolites are distinguishable in ^{1}H NMR spectra at short echo time. Then, analysis with LCModel (Stephen Provencher Inc., Oakville, Ontario, Canada) or similar algorithms permits to measure several components and quantify compounds like creatine (comprising both phosphorylated and unphosphorylated forms), NAA, *myo*-inositol, total choline-containing compounds, and glutamate plus glutamine (the so called "Glx"). In a clinical 3.0 T system, Mekle et al. (2009) achieved spectral resolution sufficient to quantify a neurochemical profile composed of 14 metabolites. The same was possible at 7.0 T in half of the scan time, i.e. 4 min (Gambarota et al., 2009; Mekle et al., 2009; Tkáč et al., 2009). At 9.4 T, with a 3 min scan, the same neurochemical profile was determined (Deelchand et al., 2010). This means that, at high field, the variety of neurochemicals detected in the human brain increasingly resemble those in rodents. Therefore, this reliable tool opens a new window for diagnosing neurological disorders and monitoring therapy outcomes. Furthermore, because the exact same tool can be applied to rodents, ^{1}H NMR spectroscopy in animal models with specific neuropathological phenotypes is an excellent basis for translational research aiming to understand biochemical mechanisms of disease development and progression.

Hungtinton's disease

Huntington's disease (HD) is a neurodegenerative illness caused by a polyglutamine expansion mutation at the N-terminal end of the huntingtin protein. GABAergic medium-sized spiny neurons in the striatum are particularly affected and progressively lost with disease progression, which has been associated with mitochondrial dysfunction in both neurons and glia (e.g. Lin and Beal, 2006; Oliveira, 2010). Transgenic mice models have been created with mutated huntingtin to study the mechanisms of the disease and definitively suggest compromised mitochondrial dysfunction as a hallmark of HD (reviewed in Oliveira, 2010). The neurochemical profile of such mice reveal consistent modifications (Jenkins et al., 2000, 2005; Tkáč et al., 2007; Zacharoff et al., 2011). In the R6/2 transgenic mouse model of HD, striatal concentrations of creatine, glycerophosphorylcholine, glutamine and glutathione were found to be increased and NAA levels decreased (Jenkins et al., 2000; Tkáč et al., 2007). Further development of the disease leads to additional modifications, namely increased concentrations of phosphocreatine, taurine, ascorbate, glutamate, and *myo*-inositol and decreased phophorylethanolamine (Tkáč et al., 2007). From these alterations, reduced NAA concentration was found to be consistently related to striatal neuron dysfunction and to accentuate with progression of the disease phenotype and with polyglutamine expansion length, as well as gene expression levels and protein context (Jenkins et al., 2005). Increased GSH, ascorbate and taurine appear as counter-regulatory response HD associated oxidative stress (Choo et al., 2005). Modification of relative phospholipid levels indicate altered cell membrane turnover, which is consistent with changes in membrane properties of medium-sized spiny neurons that compromise integrity of the membrane potential (Klapstein et al., 2001). Glutamine and glutamate alterations suggest the impaired neurotransmission and glutamate–glutamine cycling, while increased creatine and phosphocreatine are the reflection of impaired mitochondrial bioenergetics and reduced oxidative phosphorylation (Oliveira, 2010). Recently, an elegant study in the R6/2 model of HD demonstrated that neurochemical alterations measured by MRS anticipate structural deterioration detectable in MR images (Zacharoff et al., 2011), indicating that the neurochemical profile may be used as biomarker for early therapeutic decisions.

Mitochondrial toxins like 3-nitropropionic acid (3-NP) and malonate, functioning as inhibitors of the complex II of mitochondrial respiratory chain, effectively induce behavioral changes and selective striatal lesions in animals mimicking symptoms of HD. In fact, like in the striatum of R6/2 transgenic mice, 3-NP-treated rats display reduced striatal NAA levels (reviewed in Lee and Chang, 2004). In accordance with the expected mitochondrial impairment, the inhibitor of the respiratory chain 3-NP leads to increased striatal lactate concentration (e.g. Jenkins et al., 1996; Lee and Chang, 2004; Tsai et al., 1997).

Parkinson's disease

Parkinson's disease (PD) is a disorder of the central nervous system associated with degeneration of dopaminergic neurons located in the ventral mesencephalon, which impairs motor skills, cognitive processes, and other mental functions. Although the mechanisms by which these neurons degenerate in PD are poorly understood, indirect evidence suggests involvement of glutamatergic mechanisms in the pathogenesis of this disorder. PD not only affects basal ganglia, the pathology is accompanied by functional changes of cerebral motor cortex. Decreased NAA to creatine ratio have been extensively observed in cerebral areas of PD patients (e.g. Camicioli et al., 2007; Lucetti et al., 2001, 2007; Taylor-Robinson et al., 1999; Tedeschi et al., 1997; reviewed by Clarke and Lowry, 2001). Lower signal corresponding to choline-containing compounds was also reported in cortical areas of PD patients (Lucetti et al., 2007; Taylor-Robinson et al., 1999). Glutamate to creatine ratio was found reduced in the anterior cingulate gyrus of PD patients in one study (Griffith et al., 2008). This particular study however failed to identify reduced NAA levels that have been frequently reported throughout different brain areas in PD. As for other neurodegenerative disorders, mitochondrial dysfunction contributes to neuronal degeneration in PD patients (Lin and Beal, 2006). Accordingly, a reduction of high-energy phosphates and increased lactate concentration was observed in several brain areas of PD patients when compared to healthy subjects (Hattingen et al., 2009; reviewed in Henchcliffe et al., 2008).

NMR spectroscopy studies in animal models of PD have been largely limited to administration of 1-methyl-4-phenyl-1,2,3,6-tetrahydropyridine (MPTP) or its active metabolite 1-methyl-4-phenylpyridinium (MPP^{+}), a neurotoxin that leads to destruction of dopaminergic neurons in the substantia nigra, causing permanent symptoms of PD (reviewed in Henchcliffe et al., 2008). Reduced NAA and increased lactate levels were observed in the striatum or substantia nigra of mouse (Boska et al., 2005; Koga et al., 2006), rat (Jenkins et al., 1996; Storey et al., 1992), feline (Podell et al., 2003), canine (Choi et al., 2011) or primate (Brownell et al., 1998) MPTP/MPP^{+}-intoxicated models, suggesting neuronal loss and mitochondrial dysfunction. GABA was suggested to be either increased (Chassain et al., 2008, 2010) of reduced (Storey et al., 1992) after MPTP/MPP^{+} treatment. Increased concentration of both glutamate and glutamine was proposed in the striatum of animal models of PD compared to controls (Chassain et al., 2008, 2010; Podell et al., 2003), as consequence of excitotoxicity and/or impaired glutamatergic neurotransmission. Rats injected with 6-hydroxydopamine and ascorbate in the substantia nigra, which also mimic phenotypes of PD, were found to have reduced NAA to creatine ratio in the frontal cortex, associated with synaptic degeneration and dopaminergic loss (Hou et al., 2010).

Amyotrophic lateral sclerosis

Amyotrophic lateral sclerosis (ALS) is a progressive neurodegenerative disease caused by the degeneration of motor neurons, thus also known as motor neuron disease. The neuronal marker NAA has

been shown to be associated to reduced neuronal integrity and neurodegeneration in ALS. Compared to healthy individuals, ALS patients show reduced levels of NAA the primary motor cortex (Gredal et al., 1997; Han and Ma, 2010; Nelles et al., 2008; Pioro et al., 1994; Pohl et al., 2001; Sarchielli et al., 2001; Suhy et al., 2002; Wang et al., 2006) and brain stem (Cwik et al., 1998; Pioro et al., 1999). Reduced NAA to total creatine ratio in motor cortex of ALS patients correlates with ALS Functional Rating Scale that depicts ALS progression (Sivák et al., 2010). Similarly, a decrease in ratio of NAA to choline-containing compounds in motor cortex is associated and correlated with disease progression in ALS patients (Pohl et al., 2001). Consistent with excitotoxicity, increased Glx levels were found in the brain stem, namely in medula oblongata (Pioro et al., 1999), and in the motor cortex (Han and Ma, 2010) of ALS patients compared to healthy subjects.

ALS patients were monitored upon treatment with riluzole and amelioration of the ratio of NAA to creatine was observed in motor cortex (Kalra et al., 1998, 2006) strengthening the hypothesis that NAA levels are a measure of neuronal integrity. Conversely, treatment with gabapentin failed to prevent neurodegeneration as depicted by a progressive decrease of NAA levels (Kalra et al., 2003). Treatment with minocycline could also prevent further decline in NAA to creatine ratio in brain stem and motor cortex, suggesting prevention of the progressive neurodegeneration (Khiat et al., 2010). However, the appropriate control group with healthy individuals was not analyzed in this particular study.

Transgenic mice with the superoxide dismutase mutation G93A have been widely utilized as an animal model of familial ALS. The brain of these mice shows reduced NAA levels (Pioro et al., 1998; Niessen et al., 2007). Increased Glx in cortical areas was also suggested by Andreassen et al. (2001). Recently, *in vivo* ^{1}H NMR spectroscopy at 9.4 T revealed that both glutamate and glutamine may be increased in brain stem, motor cortex or striatum of these mice at different stages of the disease, e.g. increased glutamate concentration followed by accumulation of glutamine (Lei et al., 2011).

Alzheimer's disease

Alzheimer's disease (AD) is a progressive neurodegenerative disorder and the most common form of dementia in elderly, occurring with increased incidence in a continuously aging population. *In vivo* ^{1}H NMR spectroscopy has opened new possibilities to assess metabolic and functional correlates of dementia in research and clinical settings, as well as prediction of future cognitive decline (Kantarci, 2007). By utilizing MRS, reduced NAA and increased *myo*-inositol concentrations have been consistently found in the brain of AD patients compared to cognitively healthy elderly individuals and to be correlated to decline in cognitive performance (e.g. Chantal et al., 2002, 2004; Huang et al., 2001; Kantarci et al., 2004; Klunk et al., 1998; Jessen et al., 2000, 2009; Meyerhoff et al., 1994; Miller et al., 1993; Mohanakrishnan et al., 1997; Pfefferbaum et al., 1999a,b; Rose et al., 1999; Schuff et al., 2002; Watanabe et al., 2010). While NAA indicates loss of neuronal integrity, *myo*-inositol has been interpreted as a marker of gliosis (see discussion above). Most of these clinical MRS studies determined NAA and *myo*-inositol contents as a ratio to other peaks in the ^{1}H NMR spectra, namely choline and creatine. However, some studies found elevated choline (Kantarci et al., 2004; Meyerhoff et al., 1994; Pfefferbaum et al., 1999a,b) and creatine (Huang et al., 2001) signals in ^{1}H NMR spectra from the brain of AD patients compared to healthy controls. Increases in GPC levels in post-mortem cortical gray matter measured analytically from severely demented AD brains have been attributed to membrane breakdown (Nitsch et al., 1992). However, choline and creatine resonances were reduced in certain brain areas of AD patients compared to controls (Chantal et al., 2002; Watanabe et al., 2010).

The concentration of NAA in brain areas of patients with mild cognitive impairment was found to be lower than that in the brains of AD patients but higher than that of healthy subjects (e.g. Jessen et al., 2009; Kantarci et al., 2007; Watanabe et al., 2010). Furthermore, NAA decrease has been suggested to correlate with cognitive decline from light dementia to AD (e.g. Chantal et al., 2002, 2004; Pilatus et al., 2009). These findings suggest a positive correlation between NAA levels and cognitive performance.

Impaired cerebral energy metabolism is known to occur in AD patients (reviewed in Ferreira et al., 2010). Accordingly, in addition to these neurochemical markers, after glucose administration, glucose is observed in the brain of AD patients at higher levels than healthy subjects (Haley et al., 2006). The increased brain glucose levels thus likely reflect reduced glucose metabolism, although the increased contribution of high concentrated glucose in CSF due to atrophy may contribute.

Gene mutations associated with early-onset familial AD directly affect amyloid metabolism (Selkoe, 1995). Namely, these are mutations associated with the β-amyloid precursor protein (APP), presenillin 1 (PS1) and presenillin 2 (PS2). Murine models of AD have been created by inserting one or more of these human mutations into the mouse genome and have been explored by *in vivo* ^{1}H NMR spectroscopy.

Double transgenic mice expressing human mutant APP and human mutated PS1 (APP/PS1) display decreased glutamate and NAA concentrations in the brain, particularly in the hippocampus, that were observed at the time where hippocampal volume was already reduced but amyloid plaques were not yet present (Choi et al., 2010; Marjanska et al., 2005; Oberg et al., 2008). Later, upon visible amyloid deposits, these mice also presented increased brain *myo*-inositol to creatine ratio, when compared to wild type mice (Jack et al, 2007), accompanied by astrogliosis as detected by histochemistry methods (Chen et al., 2009). Increased *myo*-inositol and glutamine and decreased NAA and glutamate were reported to occur in the cortex of these mice. Additionally, it was found that once amyloid plaques are observed, NAA levels are inversely associated to the area of cortex occupied by plaques (Choi et al., 2010).

Dedeoglu et al. (2004) but not Marjanska et al. (2005) reproduced these findings in mice possessing only the mutated APP gene. Both authors reported, however, higher cerebral taurine to creatine ratio in the brain of APP transgenic mice compared to wild type mice (Dedeoglu et al., 2004; Marjanska et al., 2005). These results were confirmed by *in vitro* NMR spectroscopy of brain extracts, in which glutathione levels were additionally found to be lower than in controls (Dedeoglu et al., 2004).

In summary, compared to healthy subjects, AD patients display lower NAA and increased *myo*-inositol in the brain, reflecting disease progression. These observations are also mimicked in animal models of AD. However, contradictory results have appeared regarding some metabolic observations and their regional distribution.

Hypoxic and ischemic diseases

A drop in cerebral perfusion reduces glucose and oxygen supply, thus starting a cascade of electrophysiological and metabolic events leading to cell injury, loss of function and then neurodegeneration.

Profound metabolic changes occur during ischemia and after, in early stages of re-oxygenation, some metabolic alterations persist (Berthet et al., 2011; Lei et al., 2009), particularly dramatically increased lactate levels that can be further used by neurons upon reperfusion (Berthet et al., 2009). In addition, during ischemia there is a decrease in glutamate and a transient glutamine increase, likely to be linked to the excitotoxic release of glutamate and conversion into glial glutamine. Interestingly, decreases in NAA, as well as in the osmolyte taurine, exceeded those in neuronal glutamate, suggesting that the putative neuronal marker NAA is a sensitive marker

of neuronal viability. With further ischemia evolution, additional, more profound concentration decreases are detected, reflecting a disruption of cellular function. Thus, early changes in markers of energy metabolism, glutamate excitotoxicity, osmolarity deregulation and neuronal viability can be detected with high precision non-invasively in mice after stroke, and provide a better understanding of the sequential early changes in the brain parenchyma after ischemia (Lei et al., 2009), which could be used to identify new targets for neuroprotection and defining metabolic markers of tissue viability after stroke (Berthet et al., 2011; Bruhn et al., 1989; Gideon et al., 1992, 1994).

As the neurochemical profile is modified strongly during cerebral development (Kulak et al., 2010; Tkáč et al., 2003), also the reaction to an acute injury like ischemia is distinct if occurring some days after birth or during adulthood. In rat pups after birth (at P4), ischemia triggers an acute decrease of most of the metabolite concentrations and an increase in lactate, followed by a recovery phase with minor metabolic modifications in spite of abnormal brain development (at P25) (van de Looij et al., 2011a). It was observed that the increase of lactate concentration at P4 correlated with the cortical loss at P25 (van de Looij et al., 2011a), giving insight into the early prediction of long-term cerebral alterations following a moderate insult caused by hypoxia or ischemia, which could be of interest in clinical practice.

Recurrent exposure to hypoxia periods during development leads to the establishment of chronic neurochemical alterations of a different nature, particularly aspartate, creatine, phosphocreatine, GABA, glutamate, glutamine, glutathione, *myo*-inositol, NAA, phosphorylethanolamine (Raman et al., 2005; Rao et al., 2006). The increased PCr/Cr and Glu/Gln ratios and GABA levels are consistent with decreased brain energy consumption and impaired neurotransmission. Decreased NAA and phosphorylethanolamine suggest reduced neuronal integrity and phospholipid metabolism. These hippocampal alterations suggest impaired neurochemical processes that reflect development of cognitive deficits, which are observable in infants suffering from chronic hypoxia (e.g. Kirkham and Datta, 2006).

Lactate and NAA are therefore metabolic markers of strong interest in the case of ischemic diseases. In fact, it has been shown that these markers are valuable predictors of stroke outcome and provide prognostic information complementary to imaging techniques (e.g. Gideon et al., 1994; Parsons et al., 2000; Pereira et al., 1999; Wardlaw et al., 1998). Recently, a study in experimental models of ischemia revealed neurochemical modifications, namely in NAA, glutamate and taurine concentrations, at an early time point after reperfusion, when structural abnormalities were absent and/or undetectable by MRI methods (Berthet et al., 2011). Interestingly, the type and intensity of these neurochemical modifications were strong predictors of the lesion volume measured 1 day after the ischemic insult (Berthet et al., 2011). Further research may lead to the establishment of metabolic markers in stroke patients predicting the outcome after stroke, thus facilitating appropriate therapeutic decisions based on ^{1}H NMR spectroscopy data.

Diabetic encephalopathy

Diabetes mellitus is a metabolic disease characterized by hyperglycemia and its treatment with insulin frequently results in hypoglycemia episodes. Both hyper- and hypoglycemia affect brain function and may lead to cognitive dysfunction and dementia. Experimental diabetic conditions cause deficits in spatial learning and synaptic plasticity (e.g. Biessels et al., 1996), synaptic degeneration (e.g. Duarte et al., 2006, 2009a; Grillo et al., 2005) and increased astrocyte reactivity and proliferation (e.g. Baydas et al., 2003; Saravia et al., 2002) particularly in the hippocampus, a structure involved in learning and memory processing. These structural and functional modifications are likely to lead to altered cerebral metabolism (Duarte et al., 2009a).

Duarte et al. (2009a) found that diabetic rats under chronic hyperglycemia, induced by STZ administration, display a plethora of metabolic alterations in the hippocampus, most of which are normalized upon acute restoration of euglycemia. Some of the metabolites more affected by hyperglycemia were *myo*-inositol, taurine and creatine, which are considered major organic osmolytes regulating brain osmotic adaptation, suggesting that such alterations of the neurochemical profile may be related to regulation of osmolarity. Similar results were obtained in Goto–Kakizaki rats, an experimental model of insulin resistance and type 2 diabetes (Duarte et al., 2009c). Although osmolarity regulation primarily relies on electrolytic balance, it is followed by a delayed response of organic osmolytes (e.g. Verbalis, 2010). Therefore, under chronic hyperglycemia, the accumulation of organic osmolytes in the hippocampus is suitable to avoid ion-induced perturbation of protein function. Consistent with this, a high concentration of *myo*-inositol has also been reported in the hippocampus of Zucker diabetic fatty rats compared to controls (van der Graaf et al., 2004) and in the brain of diabetes patients (Geissler et al., 2003; Kreis and Ross, 1992). Thus, the study of the neurochemical profile supports the hypothesis that hyperglycemia-induced hippocampal dysfunction mainly involves deregulation of osmotic balance rather than modification of primary metabolism. It is important to note that, although *myo*-inositol has been suggested as a marker of gliosis in several neurological disorders, in the study by Duarte et al. (2009a) it did not correlate with other markers of astrocytosis. Other studies have not detected a relation between *in vivo* cerebral myo-inositol concentrations and gliosis detected by immunohistochemical methods (Kim et al., 2005; Kunz et al., 2011). On the other hand, cerebral *myo*-inositol was found to correlate with gliosis in AD (e.g. Chen et al., 2009), thus this may be, in fact, a case where eventual strong correlations do not necessarily imply causal relationships.

Schizophrenia

Schizophrenia is a neurodevelopmental disorder with both genetic and environmental aspects, involving functional alterations on both dopaminergic and glutamatergic neurotransmission, and associated with a dysfunctional redox system (Do et al., 2009). GSH, the major cellular redox regulator and antioxidant, is decreased in cerebrospinal fluid, medial prefrontal cortex (Do et al., 2000; Matsuzawa and Hashimoto, 2011) and post mortem striatum (Yao et al., 2006) of schizophrenia patients.

Schizophrenia patients display brain metabolic alterations, particularly increased glutamine and glutamate in anterior regions of the cortex (Shirayama et al., 2010; Bustillo et al., 2009; Tayoshi et al., 2009; Lutkenhoff et al., 2008). Other reports suggested altered NAA, creatine and choline in the thalamus (Yoo et al., 2009) and hippocampus (Lutkenhoff et al., 2008).

Altered glutamatergic neurotransmission leads to altered levels of glutamine, glutamate and most notably of glutamine-to-glutamate ratio, as observed in ^{1}H NMR spectra from anterior brain areas of schizophrenia patients (Shirayama et al., 2010; Bustillo et al., 2009; Tayoshi et al., 2009; Lutkenhoff et al., 2008), and similar observations have been reported in experimental models of schizophrenia. A recent study reported elevated glutamine to glutamate ratio and changed energy metabolism in prefrontal cortex of rats with NMDA receptor hypofunction, a rodent model that mimics schizophrenia symptoms (Iltis et al., 2009).

Mice with sustained GSH deficit induced by genetic deletion of its key synthesizing enzyme, glutamate-cysteine ligase modulatory subunit, also display increased cortical glutamate, glutamine and glutamine-to-glutamate ratio, consistent with impaired glutamatergic neurotransmission, and increased NAA and *myo*-inositol, in

accordance with myelination deficits (Duarte et al., 2011), both featured in the schizophrenia brain (Do et al., 2009). Interestingly, in accordance the neurodevelopmental character of schizophrenia, these neurochemical alterations were most prominent during development and pre-pubertal age rather than in mouse adulthood (Duarte et al., 2011). In adulthood, increased cortical lactate levels were consistent with impaired mitochondrial metabolism, known to occur upon redox deregulation (Duarte et al., 2011).

Ataxia

Hereditary and sporadic neurodegenerative ataxias are a genetically and clinically heterogeneous group of movement disorders that affect particularly the cerebellum. In addition to cerebellar atrophy, clinical MRS studies have revealed that neuronal degeneration and inflammatory gliosis are associated to a decreased NAA to creatine ratio and increased *myo*-inositol to creatine ratio (Boesch et al., 2001, 2007; D'Abreu et al., 2009; França et al., 2009; Guerrini et al., 2009; Mascalchi et al., 2002; Viau et al., 2005). Recently, in a study with patients with Friedreich's ataxia and with ataxia with oculomotor apraxia type 2, absolute quantification of ^{1}H NMR spectra from the vermis showed a decrease in NAA and glutamate and an increase in *myo*-inositol and glutamine concentrations (Iltis et al., 2010). Similar observations were reported in another recent MRS study with patients affected by spinocerebellar ataxia type 1 (SCA1) (Oz et al., 2010a). This evidence for increased glutamine supports the known gliotic events. However, increased glutamine associated to reduced glutamate concentration suggests impaired glutamatergic neurotransmission. Concentrations of NAA and *myo*-inositol as well as the ratio of glutamine to glutamate in cerebellar lesions appear as the most robust biomarkers for ataxia and correlate well with ataxia scores (Iltis et al., 2010; Oz et al., 2010a,b).

Although mouse models of hereditary ataxias have been generated aiming at understanding the biochemical mechanisms of this disorder, not many studies were dedicated to the characterization of their cerebral metabolism. The neurochemical profile in the cerebellum of a mouse model of SCA1 was studied at 9.4 T (Oz et al., 2010c). In this study, compared to wild-type mice, the transgenic model presented features of the human disorder, namely reduced NAA and glutamate and increased *myo*-inositol concentrations. These modifications correlated with pathology progression as determined by behavioral and histological analyses (Oz et al., 2010c). In addition, the authors reported reduced taurine, which may be used to balance increased *myo*-inositol, and increased glucose and lactate levels (Oz et al., 2010c). In fact, higher glucose levels were found in the cerebrospinal fluid of some ataxia patients, compared to healthy subjects (Iltis et al., 2010).

To detail specific metabolic abnormalities and find robust biomarkers in clinically different ataxia types (Oz et al., 2010a,b; Viau et al., 2005), higher magnetic fields are of value for unraveling alterations in a greater number of neurochemicals in the brain of ataxia patients.

Cerebral function by dynamic ^{1}H MRS

Although *in vivo* ^{1}H NMR spectroscopy typically provides a composition of biochemicals in the brain that are often used as markers of development, differentiation and degeneration, it can be applied dynamically to evaluate cerebral functions that involve modification of metabolite concentrations. In this section, we describe some examples.

Determination of blood–brain-barrier glucose transport

Brain function relies on adequate delivery of substrate, mainly glucose and oxygen, from the blood stream. Glucose is detectable by ^{1}H NMR spectroscopy. Therefore, its transport across the blood–brain-barrier (BBB) can be measured non-invasively. Several studies have measured glucose transport and consumption by detecting brain

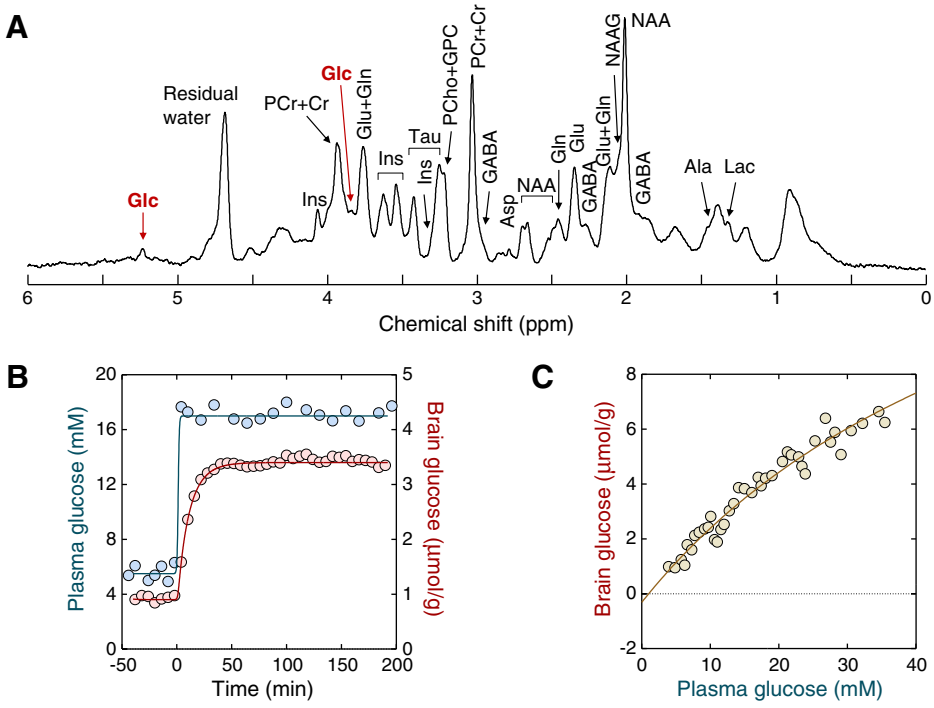

Fig. 5. Typical determination of glucose transport kinetics by *in vivo* ^{1}H NMR spectroscopy in the rat brain under α-chloralose anesthesia. Panel A shows spectrum acquired at high plasma glucose levels with glucose resonances depicted in red (Glc). Dynamic and steady-state determination of cerebral glucose transport are represented in panels B and C, respectively (see details in Duarte et al., 2009a,b).

glucose signals *in vivo* with ^{1}H NMR spectroscopy (e.g. Gruetter et al., 1996, 1998; Mason et al., 1992).

Most *in vivo* studies employing ^{1}H NMR spectroscopy to determine glucose transport across the BBB have been performed at steady-state. For that, *in vivo* ^{1}H NMR spectra are acquired at different stable glycemia levels. In these experiments, a nearly linear relation between brain and plasma glucose concentrations has been observed in humans (Gruetter et al., 1998) and in rodents (e.g. Choi et al., 2002; Duarte et al., 2009a,b; Lei et al., 2010a), within the normal physiological range. This relation was further confirmed with biochemical determination of glucose in brain extracts (comparison in Duarte et al., 2009b).

Although the kinetics can be determined from brain glucose content, the affinity constant of glucose transport is often difficult to measure (e.g. Choi et al., 2002; Lei and Gruetter, 2006; Seaquist et al., 2001) and the transport rate is determined relative to the glucose consumption rate. Thus, often a constant cerebral metabolic rate of glucose (CMR_{glc}) is assumed to determine the apparent maximal rate of glucose transport (T_{max}) (e.g. Choi et al., 2002; Duarte et al., 2009a,b; Gruetter et al., 1998; Lei et al., 2010a). However, Gruetter et al. (1996) measured glucose transport kinetics using ^{1}H NMR difference spectroscopy after a rapid increased in plasma glucose concentration, i.e. by acutely displacing glucose levels from steady-state. This method had the advantage of quantifying ^{1}H NMR spectra with only glucose resonances and allowed independent determination of both T_{max} and CMR_{glc} (Gruetter et al., 1996). Therefore, *in vivo* dynamic measurement of cerebral glucose concentration upon a challenge of plasma glucose homeostasis potentially allows distinction of both glucose transport and consumption in the brain. Typical experiments for BBB transport determination are depicted in Fig. 5.

Although glucose is the main substrate for the brain, other compounds like ketone bodies, acetate or lactate can be used as a source of energy to maintain cerebral functions when glucose supply is limiting. Because they can be detected in ^{1}H NMR spectra (Duarte et al., 2009a; Lei et al., 2010a; Xin et al., 2010b), a similar approach could be used to determine their transport rates across the BBB (e.g. Pan et al., 2001).

Functional ^{1}H NMR spectroscopy (fMRS)

Functional MRI (fMRI) measures the hemodynamic response, i.e. changes in local cerebral blood flow, blood volume and oxygenation, related to neuronal activity in the brain. In the realm of human functional studies, ^{1}H NMR spectroscopy has been used to report the time course of brain metabolites, mostly lactate, during such type of stimulation. Increase in lactate concentration was reported upon sustained visual cortex stimulation by Prichard et al. (1991), suggesting a stimulation-induced increase in cerebral metabolic rate of glucose. This observation was further confirmed (e.g. Frahm et al., 1996; Kuwabara et al., 1995; Sappey-Marinier et al., 1992) and suggested to be associated to other metabolic modifications like a decrease in glucose concentration, as detected by *in vivo* ^{1}H NMR spectroscopy (Frahm et al., 1996; Chen et al., 1993; Merboldt et al., 1992), and in phosphocreatine versus inorganic phosphate in ^{31}P NMR spectra (Sappey-Marinier et al., 1992).

With the increase in sensitivity and spectral resolution at high magnetic field, ^{1}H NMR spectroscopy in the human visual cortex allowed to detect, in addition to lactate and glucose modifications, an increase in glutamate and a decrease in aspartate levels during stimulation (Mangia et al., 2007), suggesting modifications in the flow through the malate–aspartate shuttle, possibly linked to adjustments in redox potential upon increased cerebral glucose consumption. Similar alterations of lactate, glutamate and aspartate concentrations as well as increased alanine levels have been reported in the cortex of conscious rats upon sensory stimulation (Dienel et al., 2002). However, using *in vivo* ^{1}H NMR spectroscopy in rats under α-chloralose anesthesia, Xu et al. (2005) found that sensorial stimulation could lead to an increase in glutamine and a decrease in glutamate, myo-inositol, and phosphocreatine/creatine ratio in the focally activated primary sensory cortex, albeit the modifications in lactate and glucose concentrations upon cerebral activation were not detected. ^{1}H[^{13}C] NMR spectroscopy studies upon infusion of ^{13}C-enriched glucose measured an increased tricarboxylic acid cycle flux (V_{TCA}) in focally activated primary sensory cortex during forepaw stimulation (Hyder et al., 1996, 1997; Yang and Shen, 2006) that is certainly linked to the increased cerebral metabolic rates of glucose (CMR_{glc}) and oxygen (CMR_{O2}), as well as in humans (Chen et al., 2001). Altogether, these studies indicate that the blood-oxygen-level dependence (BOLD) fMRI signal-change is associated with an increase in oxidative metabolism.

Dynamic evaluation of tumor metabolism

Brain tumors are characterized by typical neurochemical profiles that are type and grade dependent and, therefore, the beneficial association of ^{1}H NMR spectroscopy to MRI techniques may increase accuracy in diagnosis than using MRI alone (Howe and Opstad, 2003; Möller-Hartmann et al., 2002; Tate et al., 2006). Tumors are known to display increased primary metabolism and other altered metabolic fluxes, and this property has been explored as way of contributing for tumor diagnostics (Simões et al., 2008, 2010). A mouse model of glioma was challenged with acute hyperglycemia thus not only measuring the steady-state neurochemical profile but determining the reaction of the tumor to a metabolic perturbation (Simões et al., 2008). Furthermore, by using spectroscopic imaging, the response of the tumoral tissue to the metabolic challenge could be compared to the surrounding healthy tissue (Simões et al., 2010). By induction of acute simultaneous hyperglycemia and hypothermia stimuli, Simões et al. (2010) identified increased glucose levels in the tumor and heterogeneity of tumor response at the tumor center or penumbra. Similarly, with ^{13}C NMR spectroscopy upon ^{13}C-enriched glucose administration, increased glucose and lactate signals were observed in the tumor compared to non-tumor tissue (Ross et al., 1988; Terpstra et al., 1998a,b; Wijnen et al., 2010b). In these studies, reduced ^{13}C incorporation in to glutamate was observed in the tumor (Wijnen et al., 2010b) as result of reduced TCA cycle flux. All together, these observations are the result of increased BBB permeability and higher glycolytic metabolism in tumors. Further investigations are needed to identify if different tumor types and grade have specific responses to acute metabolic challenges.

Concluding remarks and future directions

NMR spectroscopy no longer admits a clinical neuroscience that is divorced from basic research, as it perfectly bridges them. ^{1}H NMR spectroscopy can be applied *in vivo* and localized in the brain to reliably detect a neurochemical profile comprising several biomarkers of interest, that can be used for diagnostic procedures and therapy monitoring due to its non-invasive character.

As depicted from the examples described above, most data from clinical studies are acquired with long echo times that lead to simplification of the acquired spectra but also cause loss of informative content in the MRS scans. In addition, many clinical cases are scanned with low spectral resolution. This, together with high inter-subject variability and often small number of scanned subjects, has possibly led to conflicting observations in the realm of CNS disorders. Conversely, by using short echo times and acquiring high quality *in vivo* ^{1}H NMR spectra, an extended neurochemical profile can be determined.

NMR spectroscopy can be further extended to spectroscopic imaging with spatial resolution in the μL range in the rodent brain, being comparable to the spatial resolution of animal PET imaging but with

the advantage of detecting simultaneously a wide range of molecules. Because pathologies affecting the CNS lead to alteration of this extended composition of neurochemicals with specific regional incidence, mapping the neurochemical profile throughout the brain using spectroscopic imaging may be of added value for diagnosis and therapy monitoring.

Acknowledgments

This work was supported by the Centre d'Imagerie BioMédicale (CIBM) of the UNIL, UNIGE, HUG, CHUV, EPFL and the Leenaards and Jeantet Foundations. The authors are grateful to Benoit Schaller and Dr. Lijing Xin who kindly provided spectra from the human brain for Fig. 3, and to Malte F. Alf for the spectroscopic images used in Fig. 2.

References

Abildgaard, F., Gesmar, H., Led, J.J., 1988. Quantitative analysis of complicated nonideal Fourier transform NMR spectra. J. Magn. Reson. 79, 78–89.
Adriany, G., Van de Moortele, P.F., Ritter, J., Moeller, S., Auerbach, E.J., Akgun, C., Snyder, C.J., Vaughan, T., Ugurbil, K., 2008. A geometrically adjustable 16-channel transmit/receive transmission line array for improved RF efficiency and parallel imaging performance at 7 Tesla. Magn. Reson. Med. 59, 590–597.
Albrecht, J., Schousboe, A., 2005. Taurine interaction with neurotransmitter receptors in the CNS: an update. Neurochem. Res. 30, 1615–1621.
Albright, C.D., Siwek, D.F., Craciunescu, C.N., Mar, M.H., Kowall, N.W., Williams, C.L., Zeisel, S.H., 2003. Choline availability during embryonic development alters the localization of calretinin in developing and aging mouse hippocampus. Nutr. Neurosci. 6 (2), 129–134.
Alf, F.M, Lei, H., Berthet, C., Hirt, L., Gruetter, R., Mlynarik, V., 2011. High-resolution spatial mapping of changes in the neurochemical profile after focal ischemia in mice. NMR Biomed. 2011 Jul 15. doi:10.1002/nbm.1740. [Epub ahead of print].
An, L., Zhang, Y., Thomasson, D.M., Latour, L.L., Baker, E.H., Shen, J., Warach, S., 2009. Measurement of glutathione in normal volunteers and stroke patients at 3 T using J-difference spectroscopy with minimized subtraction errors. J. Magn. Reson. Imaging 30, 263–270.
Anderson, S.A., Classey, J.D., Condé, F., Lund, J.S., Lewis, D.A., 1995. Synchronous development of pyramidal neuron dendritic spines and parvalbumin-immunoreactive chandelier neuron axon terminals in layer III of monkey prefrontal cortex. Neuroscience 67 (1), 7–22.
Andreassen, O.A., Jenkins, B.G., Dedeoglu, A., Ferrante, K.L., Bogdanov, M.B., Kaddurah-Daouk, R., Beal, M.F., 2001. Increases in cortical glutamate concentrations in transgenic amyotrophic lateral sclerosis mice are attenuated by creatine supplementation. J. Neurochem. 77, 383–390.
Angelie, E., Bonmartin, A., Boudraa, A., Gonnaud, P.M., Mallet, J.J., Sappey-Marinier, D., 2001. Regional differences and metabolic changes in normal aging of the human brain: proton MR spectroscopic imaging study. Am. J. Neuroradiol. 22, 119–127.
Avdievich, N.I., Oh, S., Hetherington, H.P., Collins, C.M., 2010. Improved homogeneity of the transmit field by simultaneous transmission with phased array and volume coil. J. Magn. Reson. 32, 476–481.
Ballatori, N., Krance, S.M., Notenboom, S., Shi, S., Tieu, K., Hammond, C.L., 2009. Glutathione dysregulation and the etiology and progression of human diseases. Biol. Chem. 390, 191–214.
Baslow, M.H., 2003. N-acetylaspartate in the vertebrate brain: metabolism and function. Neurochem Res 28, 941–953.
Baydas, G., Nedzvetskii, V.S., Tuzcu, M., Yasar, A., Kirichenko, S.V., 2003. Increase of glial fibrillary acidic protein and S-100B in hippocampus and cortex of diabetic rats: effects of vitamin E. Eur. J. Pharmacol. 462, 67–71.
Bayer, S.M., McMurray, W.C., 1967. The metabolism of amino acids in developing rat brain. J. Neurochem. 14, 695–706.
Behar, K.L., Rothman, D.L., Petersen, K.F., Hooten, M., Delaney, R., Petroff, O.A., Shulman, G.I., Navarro, V., Petrakis, I.L., Charney, D.S., Krystal, J.H., 1999. Preliminary evidence of low cortical GABA levels in localized ^{1}H-MR spectra of alcohol-dependent and hepatic encephalopathy patients. Am. J. Psychiatry 156, 952–954.
Benítez-Diaz, P., Miranda-Contreras, L., Mendoza-Briceño, R.V., Peña-Contreras, Z., Palacios-Prü, E., 2003. Prenatal and postnatal contents of amino acid neurotransmitters in mouse parietal cortex. Dev. Neurosci. 25, 366–374.
Berthet, C., Lei, H., Thevenet, J., Gruetter, R., Magistretti, P.J., Hirt, L., 2009. Neuroprotective role of lactate after cerebral ischemia. J. Cereb. Blood Flow Metab. 29, 1780–1789.
Berthet, C., Lei, H., Gruetter, R., Hirt, L., 2011. Early predictive biomarkers for lesion after transient cerebral ischemia. Stroke 42, 799–805.
Betz, H., Laube, B., 2006. Glycine receptors: recent insights into their structural organization and functional diversity. J. Neurochem. 97, 1600–1610.
Bielicki, G., Chassain, C., Renou, J.P., Farges, M.C., Vasson, M.P., Eschalier, A., Durif, F., 2004. Brain GABA editing by localized *in vivo* ^{1}H magnetic resonance spectroscopy. NMR Biomed. 17, 60–68.
Biessels, G.J., Kamal, A., Ramakers, G.M., Urban, I.J., Spruijt, B.M., Erkelens, D.W., Gispen, W.H., 1996. Place learning and hippocampal synaptic plasticity in streptozotocin-induced diabetic rats. Diabetes 45, 1259–1266.
Bitsch, A., Bruhn, H., Vougioukas, V., Stringaris, A., Lassmann, H., Frahm, J., Brück, W., 1999. Inflammatory CNS demyelination: histopathologic correlation with in vivo quantitative proton MR spectroscopy. AJNR Am. J. Neuroradiol. 20, 1619–1627.
Blüml, S., Seymour, K.J., Ross, B.D., 1999. Developmental changes in choline- and ethanolamine-containing compounds measured with proton-decoupled ^{31}P MRS in *in vivo* human brain. Magn. Reson. Med. 42, 643–654.
Boer, V.O., Siero, J.C., Hoogduin, H., van Gorp, J.S., Luijten, P.R., Klomp, D.W., 2011. High-field MRS of the human brain at short TE and TR. NMR Biomed 24, 1081–1088.
Boesch, C., Gruetter, R., Martin, E., 1991. Temporal and spatial analysis of fields generated by eddy currents in superconducting magnets: optimization of corrections and quantitative characterization of magnet/gradient systems. Magn. Reson. Med. 20, 268–284.
Boesch, S.M., Schocke, M., Bürk, K., Hollosi, P., Fornai, F., Aichner, F.T., Poewe, W., Felber, S., 2001. Proton magnetic resonance spectroscopic imaging reveals differences in spinocerebellar ataxia types 2 and 6. J. Magn. Reson. Imaging 13, 553–559.
Boesch, S.M., Wolf, C., Seppi, K., Felber, S., Wenning, G.K., Schocke, M., 2007. Differentiation of SCA2 from MSA-C using proton magnetic resonance spectroscopic imaging. J. Magn. Reson. Imaging 25, 564–569.
Boska, M.D., Lewis, T.B., Destache, C.J., Benner, E.J., Nelson, J.A., Uberti, M., Mosley, R.L., Gendelman, H.E., 2005. Quantitative ^{1}H magnetic resonance spectroscopic imaging determines therapeutic immunization efficacy in an animal model of Parkinson's disease. J. Neurosci. 25, 1691–1700.
Bothwell, J.H., Rae, C., Dixon, R.M., Styles, P., Bhakoo, K.K., 2001. Hypo-osmotic swelling-activated release of organic osmolytes in brain slices: implications for brain oedema *in vivo*. J. Neurochem. 77, 1632–1640.
Bottomly, P.A 1984. Selective volume method for performing localized NMR spectroscopy. US patent 4 480 228.
Bottomly, P.A., 1987. Spatial localization in NMR spectroscopy in vivo. Ann N Y Acad Sci 508, 333–348.
Bowtell, R., Mansfield, P., 1991. Gradient coil design using active magnetic screening. Magn. Reson. Med. 17, 15–19.
Brand, A., Richter-Landsberg, C., Leibfritz, D., 1993. Multinuclear NMR studies on the energy metabolism of glial and neuronal cells. Dev. Neurosci. 15, 289–298.
Brown, T.R., Kincaid, B.M., Ugurbil, K., 1982. NMR chemical shift imaging in three dimensions. Proc. Natl. Acad. Sci. U.S.A. 79, 3523–3526.
Brownell, A.L., Jenkins, B.G., Elmaleh, D.R., Deacon, T.W., Spealman, R.D., Isacson, O., 1998. Combined PET/MRS brain studies show dynamic and long-term physiological changes in a primate model of Parkinson disease. Nat. Med. 4, 1308–1312.
Bruhn, H., Frahm, J., Gyngell, M.L., Merboldt, K.D., Hänicke, W., Sauter, R., 1989. Cerebral metabolism in man after acute stroke: new observations using localized proton NMR spectroscopy. Magn. Reson. Med. 9, 126–131.
Brulatout, S., Méric, P., Loubinoux, I., Borredon, J., Corrèze, J.L., Roucher, P., Gillet, B., Bérenger, G., Beloeil, J.C., Tiffon, B., Mispelter, J., Seylaz, J., 1996. A one-dimensional (proton and phosphorus) and two-dimensional (proton) *in vivo* NMR spectroscopic study of reversible global cerebral ischemia. J. Neurochem. 66, 2491–2499.
Burlina, A.P., Skaper, S.D., Mazza, M.R., Ferrari, V., Leon, A., Burlina, A.B., 1994. *N*-acetylaspartylglutamate selectively inhibits neuronal responses to *N*-methyl-D-aspartic acid *in vitro*. J. Neurochem. 63, 1174–1177.
Burri, R., Bigler, P., Straehl, P., Posse, S., Colombo, J.P., Herschkowitz, N., 1990. Brain development: ^{1}H magnetic resonance spectroscopy of rat brain extracts compared with chromatographic methods. Neurochem. Res. 15, 1009–1016.
Burri, R., Steffen, C., Herschkowitz, N., 1991. *N*-acetyl-L-aspartate is a major source of acetyl groups for lipid synthesis during rat brain development. Dev. Neurosci. 13, 403–411.
Bustillo, J.R., Rowland, L.M., Mullins, P., Jung, R., Chen, H., Qualls, C., Hammond, R., Brooks, W.M., Lauriello, J., 2009. ^{1}H-MRS at 4 Tesla in minimally treated early schizophrenia. Mol. Psychiatry 15 (6), 629–636.
Camicioli, R.M., Hanstock, C.C., Bouchard, T.P., Gee, M., Fisher, N.J., Martin, W.R., 2007. Magnetic resonance spectroscopic evidence for presupplementary motor area neuronal dysfunction in Parkinson's disease. Mov. Disord. 22, 382–386.
Cassidy, M., Neale, J.H., 1993. *N*-Acethylaspartylglutamate catabolism is achieved by an enzyme on the cell surface of neurons and glia. Neuropeptides 24, 271–278.
Castro, M.A., Beltran, F.A., Brauchi, S., Concha, I.I., 2009. A metabolic switch in brain: glucose and lactate metabolism modulation by ascorbic acid. J. Neurochem. 110, 423–440.
Cerdan, S., Künnecke, B., Seelig, J., 1990. Cerebral metabolism of [1,2-$^{13}C_2$]acetate as detected by *in vivo* and *in vitro* ^{13}C NMR. J. Biol. Chem. 265, 12916–12926.
Chakraborty, G., Mekala, P., Yahya, D., Wu, G., Ledeen, R.W., 2001. Intraneuronal *N*-acetylaspartate supplies acetyl groups for myelin lipid synthesis: evidence for myelin-associated aspartoacylase. J. Neurochem. 78, 736–745.
Chang, L., Ernst, T., Poland, R.E., Jenden, D.J., 1996. *In vivo* proton magnetic resonance spectroscopy of the normal aging human brain. Life Sci. 58, 2049–2056.
Chantal, S., Labelle, M., Bouchard, R.W., Braun, C.M., Boulanger, Y., 2002. Correlation of regional proton magnetic resonance spectroscopic metabolic changes with cognitive deficits in mild Alzheimer disease. Arch. Neurol. 59, 955–962.
Chantal, S., Braun, C.M., Bouchard, R.W., Labelle, M., Boulanger, Y., 2004. Similar 1H magnetic resonance spectroscopic metabolic pattern in the medial temporal lobes of patients with mild cognitive impairment and Alzheimer disease. Brain Res. 1003, 26–35.
Chassain, C., Bielicki, G., Durand, E., Lolignier, S., Essafi, F., Traoré, A., Durif, F., 2008. Metabolic changes detected by proton magnetic resonance spectroscopy *in vivo* and *in vitro* in a murin model of Parkinson's disease, the MPTP-intoxicated mouse. J. Neurochem. 105, 874–882.
Chassain, C., Bielicki, G., Keller, C., Renou, J.P., Durif, F., 2010. Metabolic changes detected *in vivo* by ^{1}H MRS in the MPTP-intoxicated mouse. NMR Biomed. 23, 547–553.

Chen, W., Novotny, E.J., Zhu, X.H., Rothman, D.L., Shulman, R.G., 1993. Localized 1H NMR measurement of glucose consumption in the human brain during visual stimulation. Proc. Natl. Acad. Sci. U.S.A. 90, 9896–9900.

Chen, W., Zhu, X.H., Gruetter, R., Seaquist, E.R., Adriany, G., Ugurbil, K., 2001. Study of tricarboxylic acid cycle flux changes in human visual cortex during hemifield visual stimulation using 1H-[13C] MRS and fMRI. Magn. Reson. Med. 45, 349–355.

Chen, S.Q., Wang, P.J., Ten, G.J., Zhan, W., Li, M.H., Zang, F.C., 2009. Role of myo-inositol by magnetic resonance spectroscopy in early diagnosis of Alzheimer's disease in APP/PS1 transgenic mice. Dement. Geriatr. Cogn. Disord. 28, 558–566.

Choi, I.Y., Lei, H., Gruetter, R., 2002. Effect of deep pentobarbital anesthesia on neurotransmitter metabolism in vivo: on the correlation of total glucose consumption with glutamatergic action. J. Cereb. Blood Flow Metab. 22, 1343–1351.

Choi, I.Y., Lee, S.P., Shen, J., 2005. Selective homonuclear Hartmann–Hahn transfer method for *in vivo* spectral editing in the human brain. Magn. Reson. Med. 53, 503–510.

Choi, J.K., Jenkins, B.G., Carreras, I., Kaymakcalan, S., Cormier, K., Kowall, N.W., Dedeoglu, A., 2010. Anti-inflammatory treatment in AD mice protects against neuronal pathology. Exp. Neurol. 223, 377–384.

Choi, C.B., Kim, S.Y., Lee, S.H., Jahng, G.H., Kim, H.Y., Choe, B.Y., Ryu, K.N., Yang, D.M., Yim, S.V., Choi, W.S., 2011. Assessment of metabolic changes in the striatum of a MPTP-intoxicated canine model: *in vivo* ^{1}H-MRS study of an animal model for Parkinson's disease. Magn. Reson. Imaging 29, 32–39.

Choo, Y.S., Mao, Z., Johnson, G.V., Lesort, M., 2005. Increased glutathione levels in cortical and striatal mitochondria of the R6/2 Huntington's disease mouse model. Neurosci. Lett. 386, 63–68.

Clarke, C.E., Lowry, M., 2001. Systematic review of proton magnetic resonance spectroscopy of the striatum in parkinsonian syndromes. Eur. J. Neurol. 8, 573–577.

Córdoba, J., Sanpedro, F., Alonso, J., Rovira, A., 2002. ^{1}H magnetic resonance in the study of hepatic encephalopathy in humans. Metab. Brain Dis. 17, 415–429.

Costantino-Ceccarini, E., Morell, P., 1972. Biosynthesis of brain sphingolipids and myelin accumulation in the mouse. Lipids 7, 656–659.

Craciunescu, C.N., Albright, C.D., Mar, M.H., Song, J., Zeisel, S.H., 2003. Choline availability during embryonic development alters progenitor cell mitosis in developing mouse hippocampus. J. Nutr. 133 (11), 3614–3618.

Cudalbu, C., Mlynarik, V., Xin, L., Gruetter, R., 2009. Comparison of T_1 relaxation times of the neurochemical profile in rat brain at 9.4 Tesla and 14.1 Tesla. Magn. Reson. Med. 62, 862–867.

Cudalbu, C., Lanz, B., Duarte, J.M., Morgenthaler, F.D., Pilloud, Y., Mlynárik, V., Gruetter, R., 2011. Cerebral glutamine metabolism under hyperammonemia determined in vivo by localized (1)H and (15)N NMR spectroscopy. J Cereb Blood Flow Metab. 2011 Dec 14. doi:10.1038/jcbfm.2011.173. [Epub ahead of print].

Cvoro, V., Wardlaw, J.M., Marshall, I., Armitage, P.A., Rivers, C.S., Bastin, M.E., Carpenter, T.K., Wartolowska, K., Farrall, A.J., Dennis, M.S., 2009. Associations between diffusion and perfusion parameters, N-acetyl aspartate, and lactate in acute ischemic stroke. Stroke 40, 767–772.

Cwik, V.A., Hanstock, C.C., Allen, P.S., Martin, W.R., 1998. Estimation of brainstem neuronal loss in amyotrophic lateral sclerosis with *in vivo* proton magnetic resonance spectroscopy. Neurology 50, 72–77.

D'Abreu, A., França Jr., M., Appenzeller, S., Lopes-Cendes, I., Cendes, F., 2009. Axonal dysfunction in the deep white matter in Machado–Joseph disease. J. Neuroimaging 19, 9–12.

D'Adamo Jr., A.F., Yatsu, F.M., 1966. Acetate metabolism in the nervous system. N-acetyl-L-aspartic acid and the biosynthesis of brain lipids. J. Neurochem. 13, 961–965.

de Graaf, R.A., 2008. *In vivo* NMR spectroscopy, Principles and Techniques, Second edition. John Wiley, Chichester.

De Graaf, A.A., Bovee, W.M., 1990. Improved quantification of *in vivo* ^{1}H NMR spectra by optimization of signal acquisition and processing and by incorporation of prior knowledge into the spectral fitting. Magn. Reson. Med. 15, 305–319.

de Graaf, R.A., Brown, P.B., McIntyre, S., Nixon, T.W., Behar, K.L., Rothman, D.L., 2006. High magnetic field water and metabolite proton T_1 and T_2 relaxation in rat brain *in vivo*. Magn. Reson. Med. 56, 386–394.

de Graaf, R.A., Chowdhury, G.M.I., Behar, K.L., 2011. Quantification of high-resolution ^{1}H NMR spectra from rat brain extracts. Anal. Chem. 83, 216–224.

De Stefano, N., Matthews, P.M., Arnold, D.L., 1995. Reversible decreases in *N*-acetylaspartate after acute brain injury. Magn. Reson. Med. 34, 721–727.

Dedeoglu, A., Choi, J.K., Cormier, K., Kowall, N.W., Jenkins, B.G., 2004. Magnetic resonance spectroscopic analysis of Alzheimer's disease mouse brain that express mutant human APP shows altered neurochemical profile. Brain Res. 1012, 60–65.

Deelchand, D.K., Van de Moortele, P.F., Adriany, G., Iltis, I., Andersen, P., Strupp, J.P., Vaughan, J.T., Uğurbil, K., Henry, P.G., 2010. *In vivo* ^{1}H NMR spectroscopy of the human brain at 9.4 T: initial results. J. Magn. Reson. 206, 74–80.

del Olmo, N., Galarreta, M., Bustamante, J., Martín del Rio, R., Solís, J.M., 2000. Taurine-induced synaptic potentiation: role of calcium and interaction with LTP. Neuropharmacology 39, 40–54.

Dienel, G.A., Wang, R.Y., Cruz, N.F., 2002. Generalized sensory stimulation of conscious rats increases labeling of oxidative pathways of glucose metabolism when the brain glucose–oxygen uptake ratio rises. J. Cereb. Blood Flow Metab. 22, 1490–1502.

Do, K.Q., Trabesinger, A.H., Kirsten-Krüger, M., Lauer, C.J., Dydak, U., Hell, D., Holsboer, F., Boesiger, P., Cuénod, M., 2000. Schizophrenia: glutathione deficit in cerebrospinal fluid and prefrontal cortex *in vivo*. Eur. J. Neurosci. 12, 3721–3728.

Do, K.Q., Cabungcal, J.H., Frank, A., Steullet, P., Cuenod, M., 2009. Redox dysregulation, neurodevelopment, and schizophrenia. Curr. Opin. Neurobiol. 19, 220–230.

Doelken, M.T., Hammen, T., Bogner, W., Mennecke, A., Stadlbauer, A., Boettcher, U., Doerfler, A., Stefan, H., 2010. Alterations of intracerebral γ-aminobutyric acid (GABA) levels by titration with levetiracetam in patients with focal epilepsies. Epilepsia 51, 1477–1482.

Dringen, R., 2000. Metabolism and functions of glutathione in brain. Prog. Neurobiol. 62, 649–671.

Duarte, J.M.N., Oliveira, C.R., Ambrosio, A.F., Cunha, R.A., 2006. Modification of adenosine A_1 and A_{2A} receptor density in the hippocampus of streptozotocin-induced diabetic rats. Neurochem. Int. 48, 144–150.

Duarte, J.M.N., Carvalho, R.A., Cunha, R.A., Gruetter, R., 2009a. Caffeine consumption attenuates neurochemical modifications in the hippocampus of streptozotocin-induced diabetic rats. J. Neurochem. 111, 368–379.

Duarte, J.M.N., Morgenthaler, F.D., Lei, H., Poitry-Yamate, C., Gruetter, R., 2009b. Steady-state brain glucose transport kinetics re-evaluated with a four-state conformational model. Front Neuroenerg. 1, 6.

Duarte, J.M.N., Carvalho, R.A., Cunha, R.A., Gruetter, R., 2009c. Effect of long-term caffeine consumption on glucose transport and osmolarity alterations in the hippocampus of STZ-induced and Goto–Kakizaki diabetic rats: in vivo 1H MRS study at 9.4 T. Proc. Int. Soc. Magn. Reson. Med. 17, 1084.

Duarte, J.M., Kulak, A., Gholam-Razaee, M.M., Cuenod, M., Gruetter, R., Do, K.Q. N-Acetylcysteine Normalizes Neurochemical Changes in the Glutathione-Deficient Schizophrenia Mouse Model During Development.Biol Psychiatry. 2011 Sep 25. [Epub ahead of print].

Eldridge, C.F., Bunge, M.B., Wood, P.M., 1987. Differentiation of axon-related Schwann cells *in vitro*. I. Ascorbic acid regulates basal lamina assembly and myelin formation. J. Cell Biol. 105, 1023–1034.

Ferreira, I.L., Resende, R., Ferreiro, E., Rego, A.C., Pereira, C.F., 2010. Multiple defects in energy metabolism in Alzheimer's disease. Curr. Drug Targets 11, 1193–1206.

Flint, A.C., Liu, X., Kriegstein, A.R., 1998. Nonsynaptic glycine receptor activation during early neocortical development. Neuron 20, 43–53.

Frahm, J., Krüger, G., Merboldt, K.D., Kleinschmidt, A., 1996. Dynamic uncoupling and recoupling of perfusion and oxidative metabolism during focal brain activation in man. Magn. Reson. Med. 35, 143–148.

França Jr., M.C., D'Abreu, A., Yasuda, C.L., Bonadia, L.C., Santos da Silva, M., Nucci, A., Lopes-Cendes, I., Cendes, F., 2009. A combined voxel-based morphometry and 1H-MRS study in patients with Friedreich's ataxia. J. Neurol. 256, 1114–1120.

Gambarota, G., Xin, L., Perazzolo, C., Kohler, I., Mlynárik, V., Gruetter, R., 2008. *In vivo* ^{1}H NMR measurement of glycine in rat brain at 9.4 T at short echo time. Magn. Reson. Med. 60, 727–731.

Gambarota, G., Mekle, R., Xin, L., Hergt, M., van der Zwaag, W., Krueger, G., Gruetter, R., 2009. *In vivo* measurement of glycine with short echo-time ^{1}H MRS in human brain at 7 T. MAGMA 22, 1–4.

Garwood, M., Ke, Y., 1991. Symmetric pulses to induce arbitrary flip angles with compensation for rf inhomogeneity and resonance offsets. J Magn Reson 94, 511–525.

Garwood, M., DelaBarre, L., 2001. The return of the frequency sweep: designing adiabatic pulse for contemporary NMR. J. Magn. Reson. 153, 155–177.

Geissler, A., Frund, R., Scholmerich, J., Feuerbach, S., Zietz, B., 2003. Alterations of cerebral metabolism in patients with diabetes mellitus studied by proton magnetic resonance spectroscopy. Exp. Clin. Endocrinol. Diabetes 111, 421–427.

Gideon, P., Henriksen, O., Sperling, B., Christiansen, P., Olsen, T.S., Jørgensen, H.S., Arlien-Søborg, P., 1992. Early time course of *N*-acetylaspartate, creatine and phosphocreatine, and compounds containing choline in the brain after acute stroke. A proton magnetic resonance spectroscopy study. Stroke 23, 1566–1572.

Gideon, P., Sperling, B., Arlien-Søborg, P., Olsen, T.S., Henriksen, O., 1994. Long-term follow-up of cerebral infarction patients with proton magnetic resonance spectroscopy. Stroke 25, 967–973.

Ginefri, J.C., Poirier-Quinot, M., Girard, O., Darrasse, L., 2007. Technical aspects: development, manufacture and installation of a cryo-cooled HTS coil system for high resolution *in-vivo* imaging of the mouse at 1.5 T. Methods 43, 54–67.

Glanville, N.T., Byers, D.M., Cook, H.W., Spence, M.W., Palmer, F.B., 1989. Differences in the metabolism of inositol and phosphoinositides by cultured cells of neuronal and glial origin. Biochim. Biophys. Acta 1004, 169–179.

Goddard, A.W., Mason, G.F., Almai, A., Rothman, D.L., Behar, K.L., Petroff, O.A., Charney, D.S., Krystal, J.H., 2001. Reductions in occipital cortex GABA levels in panic disorder detected with ^{1}H-magnetic resonance spectroscopy. Arch. Gen. Psychiatry 58, 556–561.

Gredal, O., Rosenbaum, S., Topp, S., Karlsborg, M., Strange, P., Werdelin, L., 1997. Quantification of brain metabolites in amyotrophic lateral sclerosis by localized proton magnetic resonance spectroscopy. Neurology 48, 878–881.

Griffith, H.R., Okonkwo, O.C., O'Brien, T., Hollander, J.A., 2008. Reduced brain glutamate in patients with Parkinson's disease. NMR Biomed. 21, 381–387.

Grillo, C.A., Piroli, G.G., Wood, G.E., Reznikov, L.R., McEwen, B.S., Reagan, L.P., 2005. Immunocytochemical analysis of synaptic proteins provides new insights into diabetes-mediated plasticity in the rat hippocampus. Neuroscience 136, 477–486.

Gruber, S., Pinker, K., Riederer, F., Chmelík, M., Stadlbauer, A., Bittsanský, M., Mlynárik, V., Frey, R., Serles, W., Bodamer, O., Moser, E., 2008. Metabolic changes in the normal ageing brain: consistent findings from short and long echo time proton spectroscopy. Eur. J. Radiol. 68, 320–327.

Gruetter, R., 1993. Automatic, localized *in vivo* adjustment of all first- and second-order shim coils. Magn. Reson. Med. 29, 804–811.

Gruetter, R., Boesch, C., 1992. Fast, non-interactive shimming on spatially localized signals: *in vivo* analysis of the magnetic field along axes. J. Magn. Reson. 96, 323–334.

Gruetter, R., Tkáč, I., 2000. Field mapping without reference scan using asymmetric echo-planar techniques. Magn. Reson. Med. 43, 319–323.

Gruetter, R., Novotny, E.J., Boulware, S.D., Rothman, D.L., Shulman, R.G., 1996. ^{1}H NMR studies of glucose transport in the human brain. J. Cereb. Blood Flow Metab. 16, 427–438.

Gruetter, R., Ugurbil, K., Seaquist, E.R., 1998. Steady-state cerebral glucose concentrations and transport in the human brain. J. Neurochem. 70, 397–408.

Gruetter, R., Adriany, G., Choi, I.Y., Henry, P.G., Lei, H., Oz, G., 2003. Localized *in vivo* ^{13}C NMR spectroscopy of the brain. NMR Biomed. 16, 313–338.

Guerrini, L., Belli, G., Mazzoni, L., Foresti, S., Ginestroni, A., Della Nave, R., Diciotti, S., Mascalchi, M., 2009. Impact of cerebrospinal fluid contamination on brain

metabolites evaluation with 1H-MR spectroscopy: a single voxel study of the cerebellar vermis in patients with degenerative ataxias. J. Magn. Reson. Imaging 30, 11–17.
Gupta, R.C., D'Archivio, M., Masella, R., 2009. Taurine as drug and functional food component. In: Masella, R., Mazza, G. (Eds.), Glutathione and Sulfur Amino Acids in Human Health and Disease. John Willey and Sons.
Gyulai, L., Bolinger, L., Leigh Jr., J.S., Barlow, C., Chance, B., 1984. Phosphorylethanolamine — the major constituent of the phosphomonoester peak observed by ^{31}P-NMR on developing dog brain. FEBS Lett. 178, 137–142.
Hahn, E.L., 1950. Spin echoes. Phys. Rev. 80, 580–594.
Haley, A.P., Knight-Scott, J., Simnad, V.I., Manning, C.A., 2006. Increased glucose concentration in the hippocampus in early Alzheimer's disease following oral glucose ingestion. Magn. Reson. Imaging 24, 715–720.
Han, J., Ma, L., 2010. Study of the features of proton MR spectroscopy (1H-MRS) on amyotrophic lateral sclerosis. J. Magn. Reson. Imaging 31, 305–308.
Hattingen, E., Magerkurth, J., Pilatus, U., Mozer, A., Seifried, C., Steinmetz, H., Zanella, F., Hilker, R., 2009. Phosphorus and proton magnetic resonance spectroscopy demonstrates mitochondrial dysfunction in early and advanced. Park. Dis. 132, 3285–3297.
Henchcliffe, C., Shungu, D.C., Mao, X., Huang, C., Nirenberg, M.J., Jenkins, B.G., Beal, M.F., 2008. Multinuclear magnetic resonance spectroscopy for *in vivo* assessment of mitochondrial dysfunction in Parkinson's disease. Ann. N. Y. Acad. Sci. 1147, 206–220.
Henning, A., Schar, M., Schulte, R.F., Wilm, B., Pruessmann, K.P., Boesiger, P., 2008. SELOVS: brain MRSI localization based on highly selective T_1- and B_1-insensitive outer-volume suppression at 3 T. Magn. Reson. Med. 59, 40–51.
Hertz, L., 2006. Glutamate, a neurotransmitter — and so much more. A synopsis of Wierzba III. Neurochem. Int. 48, 416–425.
Hetherington, H.P., Chu, W.J., Goen, O., Pan, J.W., 2006. Robust fully automated shimming of the human brain for high-field ^{1}H spectroscopic imaging. Magn. Reson. Med. 56, 26–33.
Hetherington, H.P., Avdievich, N.I., Kunznetsov, Pan J.W., 2010. RF shimming for spectroscopic localization in the human brain at 7 T. Magn. Reson. Med. 63, 9–19.
Hong, S.T., Balla, D.Z., Shajan, G., Choi, C., Uğurbil, K., Pohmann, R., 2011. Enhanced neurochemical profile of the rat brain using *in vivo* ^{1}H NMR spectroscopy at 16.4 T. Magn. Reson. Med. 65, 28–34.
Horská, A., Farage, L., Bibat, G., Nagae, L.M., Kaufmann, W.E., Barker, P.B., Naidu, S., 2009. Brain metabolism in Rett syndrome: age, clinical, and genotype correlations. Ann. Neurol. 65, 90–97.
Hou, Z., Lei, H., Hong, S., Sun, B., Fang, K., Lin, X., Liu, M., Yew, D.T., Liu, S., 2010. Functional changes in the frontal cortex in Parkinson's disease using a rat model. J. Clin. Neurosci. 17, 628–633.
Hoult, D., Richards, R., 1976. The signal-to-noise ratio of the nuclear magnetic resonance experiment. J. Magn. Reson. 24, 71–85.
Howe, F.A., Opstad, K.S., 2003. ^{1}H MR spectroscopy of brain tumours and masses. NMR Biomed. 16, 123–131.
Huang, W., Alexander, G.E., Chang, L., Shetty, H.U., Krasuski, J.S., Rapoport, S.I., Schapiro, M.B., 2001. Brain metabolite concentration and dementia severity in Alzheimer's disease: a 1H MRS study. Neurology 57, 626–632.
Hyder, F., Chase, J.R., Behar, K.L., Mason, G.F., Siddeek, M., Rothman, D.L., Shulman, R.G., 1996. Increased tricarboxylic acid cycle flux in rat brain during forepaw stimulation detected with ^{1}H[^{13}C]NMR. Proc. Natl. Acad. Sci. U.S.A. 93, 7612–7617.
Hyder, F., Rothman, D.L., Mason, G.F., Rangarajan, A., Behar, K.L., Shulman, R.G., 1997. Oxidative glucose metabolism in rat brain during single forepaw stimulation: a spatially localized ^{1}H[^{13}C] nuclear magnetic resonance study. J. Cereb. Blood Flow Metab. 17, 1040–1047.
Iltis, I., Koski, D.M., Eberly, L.E., Nelson, C.D., Deelchand, D.K., Valette, J., Ugurbil, K., Lim, K.O., Henry, P.G., 2009. Neurochemical changes in the rat prefrontal cortex following acute phencyclidine treatment: an *in vivo* localized ^{1}H MRS study. NMR Biomed. 22, 737–744.
Iltis, I., Hutter, D., Bushara, K.O., Clark, H.B., Gross, M., Eberly, L.E., Gomez, C.M., Oz, G., 2010. 1H MR spectroscopy in Friedreich's ataxia and ataxia with oculomotor apraxia type 2. Brain Res. 1358, 200–210.
Jack Jr., C.R., Marjanska, M., Wengenack, T.M., Reyes, D.A., Curran, G.L., Lin, J., Preboske, G.M., Poduslo, J.F., Garwood, M., 2007. Magnetic resonance imaging of Alzheimer's pathology in the brains of living transgenic mice: a new tool in Alzheimer's disease research. Neuroscientist 13, 38–48.
Jayakumar, P.N., Srikanth, S.G., Chandrashekar, H.S., Kovoor, J.M., Shankar, S.K., Anandh, B., 2003. Pyruvate: an *in vivo* marker of cestodal infestation of the human brain on proton MR spectroscopy. J. Magn. Reson. Imaging 18, 675–680.
Jehensen, P., Westphal, M., Schuff, N., 1990. Analytical method for the compensation of eddy-current effects induced by pulsed magnetic field gradients in NMR systems J Magn Reson 90, 264–278.
Jenkins, B.G., Brouillet, E., Chen, Y.C., Storey, E., Schulz, J.B., Kirschner, P., Beal, M.F., Rosen, B.R., 1996. Non-invasive neurochemical analysis of focal excitotoxic lesions in models of neurodegenerative illness using spectroscopic imaging. J. Cereb. Blood Flow Metab. 16, 450–461.
Jenkins, B.G., Klivenyi, P., Kustermann, E., Andreassen, O.A., Ferrante, R.J., Rosen, B.R., Beal, M.F., 2000. Nonlinear decrease over time in *N*-acetyl aspartate levels in the absence of neuronal loss and increases in glutamine and glucose in transgenic Huntington's disease mice. J. Neurochem. 74, 2108–2119.
Jenkins, B.G., Andreassen, O.A., Dedeoglu, A., Leavitt, B., Hayden, M., Borchelt, D., Ross, C.A., Ferrante, R.J., Beal, M.F., 2005. Effects of CAG repeat length, HTT protein length and protein context on cerebral metabolism measured using magnetic resonance spectroscopy in transgenic mouse models of Huntington's disease. J. Neurochem. 95, 553–562.
Jessen, F., Block, W., Träber, F., Keller, E., Flacke, S., Papassotiropoulos, A., Lamerichs, R., Heun, R., Schild, H.H., 2000. Proton MR spectroscopy detects a relative decrease of N-acetylaspartate in the medial temporal lobe of patients with AD. Neurology 55, 684–688.
Jessen, F., Gür, O., Block, W., Ende, G., Frölich, L., Hammen, T., Wiltfang, J., Kucinski, T., Jahn, H., Heun, R., Maier, W., Kölsch, H., Kornhuber, J., Träber, F., 2009. A multicenter 1H-MRS study of the medial temporal lobe in AD and MCI. Neurology 72, 1735–1740.
Kaiser, L.G., Marjańska, M., Matson, G.B., Iltis, I., Bush, S.D., Soher, B.J., Mueller, S., Young, K., 2010. ^{1}H MRS detection of glycine residue of reduced glutathione *in vivo*. J. Magn. Reson. 202, 259–266.
Kalra, S., Cashman, N.R., Genge, A., Arnold, D.L., 1998. Recovery of N-acetylaspartate in corticomotor neurons of patients with ALS after riluzole therapy. Neuroreport 9, 1757–1761.
Kalra, S., Cashman, N.R., Caramanos, Z., Genge, A., Arnold, D.L., 2003. Gabapentin therapy for amyotrophic lateral sclerosis: lack of improvement in neuronal integrity shown by MR spectroscopy. AJNR Am. J. Neuroradiol. 24, 476–480.
Kalra, S., Tai, P., Genge, A., Arnold, D.L., 2006. Rapid improvement in cortical neuronal integrity in amyotrophic lateral sclerosis detected by proton magnetic resonance spectroscopic imaging. J. Neurol. 253, 1060–1063.
Kantarci, K., 2007. ^{1}H magnetic resonance spectroscopy in dementia. Br. J. Radiol. 80, S146–S152.
Kantarci, K., Petersen, R.C., Boeve, B.F., Knopman, D.S., Tang-Wai, D.F., O'Brien, P.C., Weigand, S.D., Edland, S.D., Smith, G.E., Ivnik, R.J., Ferman, T.J., Tangalos, E.G., Jack Jr., C.R., 2004. 1H MR spectroscopy in common dementias. Neurology 63, 1393–1398.
Kantarci, K., Weigand, S.D., Petersen, R.C., Boeve, B.F., Knopman, D.S., Gunter, J., Reyes, D., Shiung, M., O'Brien, P.C., Smith, G.E., Ivnik, R.J., Tangalos, E.G., Jack Jr., C.R., 2007. Longitudinal 1H MRS changes in mild cognitive impairment and Alzheimer's disease. Neurobiol. Aging 28, 1330–1339.
Katscher, U., Bornert, P., Leussler, C., van den Brink, J.S., 2003. Transmit SENSE. Magn. Reson. Med. 49, 144–150.
Katscher, U., Rohrs, J., Bornert, P., 2005. Basic considerations on the impact of the coil array on the performance of transmit SENSE. MAGMA 18, 81–88.
Ke, Y., Streeter, C.C., Nassar, L.E., Sarid-Segal, O., Hennen, J., Yurgelun-Todd, D.A., Awad, L.A., Rendall, M.J., Gruber, S.A., Nason, A., Mudrick, M.J., Blank, S.R., Meyer, A.A., Knapp, C., Ciraulo, D.A., Renshaw, P.F., 2004. Frontal lobe GABA levels in cocaine dependence: a two-dimensional, J-resolved magnetic resonance spectroscopy study. Psychiatry Res. 130, 283–293.
Khiat, A., D'Amour, M., Souchon, F., Boulanger, Y., 2010. MRS study of the effects of minocycline on markers of neuronal and microglial integrity in ALS. Magn. Reson. Imaging 28, 1456–1460.
Kickler, N., van der Zwaag, W., Merkle, R., Kober, T., Marques, J.P., Krueger, G., Gruetter, R., 2010. Eddy current effects on a clinical 7 T–68 cm bore scanner. MAGMA 23, 39–43.
Kim, J.P., Lentz, M.R., Westmoreland, S.V., Greco, J.B., Ratai, E.M., Halpern, E., Lackner, A.A., Masliah, E., González, R.G., 2005. Relationships between astrogliosis and ^{1}H MR spectroscopic measures of brain choline/creatine and *myo*-inositol/creatine in a primate model. AJNR Am. J. Neuroradiol. 26, 752–759.
Kinoshita, Y., Yokota, A., 1997. Absolute concentrations of metabolites in human brain tumors using *in vitro* proton magnetic resonance spectroscopy. NMR Biomed. 10, 2–12.
Kirkham, F.J., Datta, A.K., 2006. Hypoxic adaptation during development: relation to pattern of neurological presentation and cognitive disability. Dev. Sci. 9, 411–427.
Kirmani, B.F., Jacobowitz, D.M., Kallarakal, A.T., Namboodiri, M.A., 2002. Aspartoacylase is restricted primarily to myelin synthesizing cells in the CNS: therapeutic implications for Canavan disease. Brain Res. Mol. Brain Res. 107, 176–182.
Klapstein, G.J., Fisher, R.S., Zanjani, H., Cepeda, C., Jokel, E.S., Chesselet, M.F., Levine, M.S., 2001. Electrophysiological and morphological changes in striatal spiny neurons in R6/2 Huntington's disease transgenic mice. J. Neurophysiol. 86, 2667–2677.
Klein, J., 2000. Membrane breakdown in acute and chronic neurodegeneration: focus on choline-containing phospholipids. J. Neural Transm. 107, 1027–1063.
Klunk, W.E., Panchalingam, K., McClure, R.J., Stanley, J.A., Pettegrew, J.W., 1998. Metabolic alterations in postmortem Alzheimer's disease brain are exaggerated by Apo-E4. Neurobiol. Aging 19, 511–515.
Koga, K., Mori, A., Ohashi, S., Kurihara, N., Kitagawa, H., Ishikawa, M., Mitsumoto, Y., Nakai, M., 2006. ^{1}H MRS identifies lactate rise in the striatum of MPTP-treated C57BL/6 mice. Eur. J. Neurosci. 23, 1077–1081.
Kohli, A., Gupta, R.K., Poptani, H., Roy, R., 1995. *In vivo* proton magnetic resonance spectroscopy in a case of intracranial hydatid cyst. Neurology 45, 562–564.
Koller, K.J., Coyle, J.T., 1984. Ontogenesis of *N*-acetyl-aspartate and *N*-acetyl-aspartyl-glutamate in rat brain. Brain Res. 317, 137–140.
Kreis, R., Ross, B.D., 1992. Cerebral metabolic disturbances in patients with subacute and chronic diabetes mellitus: detection with proton MR spectroscopy. Radiology 184, 123–130.
Kreis, R., Farrow, N., Ross, B.D., 1991. Localized ^{1}H NMR spectroscopy in patients with chronic hepatic encephalopathy. Analysis of changes in cerebral glutamine, choline and inositols. NMR Biomed. 4, 109–116.
Kreis, R., Ernst, T., Ross, B.D., 1993. Development of the human brain: *in vivo* quantification of metabolite and water content with proton magnetic resonance spectroscopy. Magn. Reson. Med. 30, 424–437.
Kulak, A., Duarte, J.M., Do, K.Q., Gruetter, R., 2010. Neurochemical profile of the developing mouse cortex determined by in vivo 1H NMR spectroscopy at 14.1 T and the effect of recurrent anaesthesia. J Neurochem 115(6):1466-77.
Kunz, N., Camm, E.J., Somm, E., Lodygensky, G., Darbre, S., Aubert, M.L., Hüppi, P.S., Sizonenko, S.V., Gruetter, R., 2011. Developmental and metabolic brain alterations in rats exposed to bisphenol A during gestation and lactation. Int. J. Dev. Neurosci. 29, 37–43.

Kuwabara, T., Watanabe, H., Tsuji, S., Yuasa, T., 1995. Lactate rise in the basal ganglia accompanying finger movements: a localized ^{1}H-MRS study. Brain Res. 670, 326–328.
Kwok, W.E., You, Z., 2006. *In vivo* MRI using liquid nitrogen cooled phasaed array coil at 3.0 T. Magn. Reson. Imaging 24, 819–823.
Lahoya, J.L., Benavides, J., Ugarte, M., 1980. Glycine metabolism and glycine synthase activity during the postnatal development of rat brain. Dev. Neurosci. 3, 75–80.
Lee, W.T., Chang, C., 2004. Magnetic resonance imaging and spectroscopy in assessing 3-nitropropionic acid-induced brain lesions: an animal model of Huntington's disease. Prog. Neurobiol. 72, 87–110.
Lei, H., Gruetter, R., 2006. Effect of chronic hypoglycaemia on glucose concentration and glycogen content in rat brain: a localized ^{13}C NMR study. J. Neurochem. 99, 260–268.
Lei, H., Mlynárik, V., Just, N., Gruetter, R., 2008. Snapshot gradient-recalled echo-planar images with very long echo time of rat brain at 9.4-T. Magn. Reson. Imaging 26, 954–960.
Lei, H., Berthet, C., Hirt, L., Gruetter, R., 2009. Evolution of the neurochemical profile after transient focal cerebral ischemia in the mouse brain. J. Cereb. Blood Flow Metab. 29, 811–819.
Lei, H., Duarte, J.M.N., Mlynarik, V., Python, A., Gruetter, R., 2010a. Deep thiopental anesthesia alters steady-state glucose homeostasis but not the neurochemical profile of rat cortex. J. Neurosci. Res. 88, 413–419.
Lei, H., Poitry-Yamate, C., Preitner, F., Thorens, B., Gruetter, R., 2010b. Neurochemical profile of the mouse hypothalamus using *in vivo* ^{1}H MRS at 14.1 T. NMR Biomed. 23, 578–583.
Lei, H., Dirren, E., Poitry-Yamate, C., Schneider, B.L., Aebishcer, P., Gruetter, R., 2011. Early metabolic changes in the amyotrophic lateral sclerosis SOD1 mouse brain are revealed using 1H MRS rather than CASL and 18FDG PET. Proceedings 19th Scientific Meeting of the International Society for Magnetic Resonance in Medicine, p. 2284.
Li, Y., Chen, A.P., Crane, J.C., Chang, S.M., Vigneron, D.B., Nelson, S.J., 2007. Three-dimensional J-resolved H-1 magnetic resonance spectroscopic imaging of volunteers and patients with brain tumors at 3 T. Magn. Reson. Med. 58, 886–892.
Lin, M.T., Beal, M.F., 2006. Mitochondrial dysfunction and oxidative stress in neurodegenerative diseases. Nature 443, 787–795.
Löbel, U., Ellison, D.W., Shulkin, B.L., Patay, Z., 2011. Infiltrative cerebellar ganglioglioma: conventional and advanced MRI, proton MR spectroscopic, and FDG PET findings in an 18-month-old child. Clin. Radiol. 66, 194–201.
Lucetti, C., Del Dotto, P., Gambaccini, G., Bernardini, S., Bianchi, M.C., Tosetti, M., Bonuccelli, U., 2001. Proton magnetic resonance spectroscopy (^{1}H-MRS) of motor cortex and basal ganglia in *de novo* Parkinson's disease patients. Neurol. Sci. 22, 69–70.
Lucetti, C., Del Dotto, P., Gambaccini, G., Ceravolo, R., Logi, C., Berti, C., Rossi, G., Bianchi, M.C., Tosetti, M., Murri, L., Bonuccelli, U., 2007. Influences of dopaminergic treatment on motor cortex in Parkinson disease: a MRI/MRS study. Mov. Disord. 22, 2170–2175.
Lust, W.D., Pundik, S., Zechel, J., Zhou, Y., Buczek, M., Selman, W.R., 2003. Changing metabolic and energy profiles in the fetal, neonatal, and adult rat brain. Metab. Brain Dis. 18, 195–206.
Lutkenhoff, E.S., van Erp, T.G., Thomas, M.A., Therman, S., Manninen, M., Huttunen, M.O., Kapiro, J., Lönnqvist, J., O'Neill, J., Cannon, T.D., 2008. Proton MRS in twin pairs discordant for schizophrenia. Mol. Psychiatry 15 (3), 308–318.
Lykkesfeldt, J., 2002. Increased oxidative damage in vitamin C deficiency is accompanied by induction of ascorbic acid recycling capacity in young but not mature guinea pigs. Free Radic. Res. 36, 567–574.
Lykkesfeldt, J., Trueba, G.P., Poulsen, H.E., Christen, S., 2007. Vitamin C deficiency in weanling guinea pigs: differential expression of oxidative stress and DNA repair in liver and brain. Br. J. Nutr. 98, 1116–1119.
Lynch, G.W., 2004. Molecular structure and function of the glycine receptor chloride channel. Physiol. Rev. 84, 1051–1095.
Ma, Q.Y., Chan, K.C., Kacher, D.F., Gao, E., Chow, M.S., Wong, K.K., Xu, H., Yang, E.S., Miller, J.R., Jolesz, F.A., 2003. Superconducting RF coils for clinical MR imaging at low field. Acad. Radiol. 10, 978–987.
Mangia, S., Tkác, I., Gruetter, R., Van de Moortele, P.F., Maraviglia, B., Uğurbil, K., 2007. Sustained neuronal activation raises oxidative metabolism to a new steady-state level: evidence from ^{1}H NMR spectroscopy in the human visual cortex. J. Cereb. Blood Flow Metab. 27, 1055–1063.
Manos, P., Bryan, G.K., Edmond, J., 1991. Creatine kinase activity in postnatal rat brain development and in cultured neurons, astrocytes, and oligodendrocytes. J. Neurochem. 56, 2101–2107.
Mansfield, P., Chapman, B., 1986. Active magnetic screening of gradient coils in NMR imaging. J. Magn. Reson. 66, 573–576.
Marjanska, M., Curran, G.L., Wengenack, T.M., Henry, P.G., Bliss, R.L., Poduslo, J.F., Jack Jr., C.R., Ugurbil, K., Garwood, M., 2005. Monitoring disease progression in transgenic mouse models of Alzheimer's disease with proton magnetic resonance spectroscopy. Proc. Natl. Acad. Sci. U.S.A. 102, 11906–11910.
Martin, H.L., Teismann, P., 2009. Glutathione — a review on its role and significance in Parkinson's disease. FASEB J. 23, 3263–3272.
Mascalchi, M., Cosottini, M., Lolli, F., Salvi, F., Tessa, C., Macucci, M., Tosetti, M., Plasmati, R., Ferlini, A., Tassinari, C.A., Villari, N., 2002. Proton MR spectroscopy of the cerebellum and pons in patients with degenerative ataxia. Radiology 223, 371–378.
Mason, G.F., Behar, K.L., Rothman, D.L., Shulman, R.G., 1992. NMR determination of intracerebral glucose concentration and transport kinetics in rat brain. J. Cereb. Blood Flow Metab. 12, 448–455.
Matsuzawa, D., Hashimoto, K., 2011. Magnetic resonance spectroscopy study of the antioxidant defense system in schizophrenia. Antioxid. Redox Signal.. doi:10.1089/ars.2010.3453 epub ahead of print 4 December 2010.
McKenna, M.C., 2007. The glutamate–glutamine cycle is not stoichiometric: fates of glutamate in brain. J. Neurosci. Res. 85, 3347–3358.
Mekle, R., Mlynárik, V., Gambarota, G., Hergt, M., Krueger, G., Gruetter, R., 2009. MR spectroscopy of the human brain with enhanced signal intensity at ultrashort echo times on a clinical platform at 3 T and 7 T. Magn. Reson. Med. 61, 1279–1285.
Merboldt, K.D., Bruhn, H., Hänicke, W., Michaelis, T., Frahm, J., 1992. Decrease of glucose in the human visual cortex during photic stimulation. Magn. Reson. Med. 25, 187–194.
Mescher, M., Merkle, H., Kirsch, J., Garwood, M., Gruetter, R., 1998. Simultaneous *in vivo* spectral editing and water suppression. NMR Biomed. 11, 266–272.
Meyerhoff, D.J., MacKay, S., Constans, J.M., Norman, D., Van Dyke, C., Fein, G., Weiner, M.W., 1994. Axonal injury and membrane alterations in Alzheimer's disease suggested by in vivo proton magnetic resonance spectroscopic imaging. Ann. Neurol. 36, 40–47.
Miller, B.L., Moats, R.A., Shonk, T., Ernst, T., Woolley, S., Ross, B.D., 1993. Alzheimer disease: depiction of increased cerebral myo-inositol with proton MR spectroscopy. Radiology 187, 433437.
Miyasaka, N., Takahashi, K., Heterington, H.P., 2006. Fully automated shim mapping method for spectroscopic imaging of the mouse brain at 11.7 Tesla. Magn. Reson. Med. 55, 198–202.
Mlynárik, V., Gambarota, G., Frenkel, H., Gruetter, R., 2006. Localized short-echo-time proton MR spectroscopy with full signal-intensity acquisition. Magn. Reson. Med. 56, 965–970.
Mlynárik, V., Cudalbu, C., Xin, L., Gruetter, R., 2008a. ^{1}H NMR spectroscopy of rat brain *in vivo* at 14.1 Tesla: improvements in quantification of the neurochemical profile. J. Magn. Reson. 194, 163–168.
Mlynárik, V., Kohler, I., Gambarota, G., Vaslin, A., Clarke, P.G., Gruetter, R., 2008b. Quantitative proton spectroscopic imaging of the neurochemical profile in rat brain with microliter resolution at ultra-short echo times. Magn. Reson. Med. 59, 52–58.
Mohanakrishnan, P., Fowler, A.H., Vonsattel, J.P., Jolles, P.R., Husain, M.M., Liem, P., Myers, L., Komoroski, R.A., 1997. Regional metabolic alterations in Alzheimer's disease: an in vitro 1H NMR study of the hippocampus and cerebellum. J. Gerontol. Series A Biol. Sci. Med. Sci. 52, B111–B117.
Möller-Hartmann, W., Herminghaus, S., Krings, T., Marquardt, G., Lanfermann, H., Pilatus, U., Zanella, F.E., 2002. Clinical application of proton magnetic resonance spectroscopy in the diagnosis of intracranial mass lesions. Neuroradiology 44, 371–381.
Mukherjee, P., Bahn, M.M., McKinstry, R.C., Shimony, J.S., Cull, T.S., Akbudak, E., Snyder, A.Z., Conturo, T.E., 2000. Differences between gray matter and white matter water diffusion in stroke: diffusion-tensor MR imaging in 12 patients. Radiology 215, 211–220.
Muse, E.D., Jurevics, H., Toews, A.D., Matsushima, G.K., Morell, P., 2001. Parameters related to lipid metabolism as markers of myelination in mouse brain. J. Neurochem. 76, 77–86.
Naressi, A., Couturier, C., Devos, J.M., Janssen, M., Mangeat, C., de Beer, R., Graveron-Demilly, D., 2001. Java-based graphical user interface for the MRUI quantitation package. MAGMA 12, 141–152.
Nehlig, A., 2004. Brain uptake and metabolism of keton bodies in animal models. Prostaglandins Leukot. Essent. Fatty Acids 70, 265–275.
Nelles, M., Block, W., Träber, F., Wüllner, U., Schild, H.H., Urbach, H., 2008. Combined 3 T diffusion tensor tractography and 1H-MR spectroscopy in motor neuron disease. AJNR Am. J. Neuroradiol. 29, 1708–1714.
Niessen, H.G., Debska-Vielhaber, G., Sander, K., Angenstein, F., Ludolph, A.C., Hilfert, L., Willker, W., Leibfritz, D., Heinze, H.J., Kunz, W.S., Vielhaber, S., 2007. Metabolic progression markers of neurodegeneration in the transgenic G93A-SOD1 mouse model of amyotrophic lateral sclerosis. Eur. J. Neurosci. 25, 1669–1677.
Nitsch, R.M., Blusztajn, J.K., Pittas, A.G., Slack, B.E., Growdon, J.H., Wurtman, R.J., 1992. Evidence for a membrane defect in Alzheimer disease brain. Proc. Natl. Acad. Sci. U.S.A. 89, 1671–1675.
Oberg, J., Spenger, C., Wang, F.H., Andersson, A., Westman, E., Skoglund, P., Sunnemark, D., Norinder, U., Klason, T., Wahlund, L.O., Lindberg, M., 2008. Age related changes in brain metabolites observed by 1H MRS in APP/PS1 mice. Neurobiol. Aging 29, 1423–1433.
Oliveira, J.M., 2010. Mitochondrial bioenergetics and dynamics in Huntington's disease: tripartite synapses and selective striatal degeneration. J. Bioenerg. Biomembr. 42, 227–234.
Ordidge, R.J., Connelly, A., Lohman, J.A., 1986. Image-selected *in vivo* spectroscopy (ISIS). A new technique for spatially selective NMR spectroscopy. J. Magn. Reson. 66, 283–294.
Oz, G., Tkáč, I., 2011. Short-echo, single-shot, full-intensity proton magnetic resonance spectroscopy for neurochemical profiling at 4 T: validation in the cerebellum and brainstem. Magn Reson Med 65, 901–910.
Oz, G., Terpstra, M., Tkác, I., Aia, P., Lowary, J., Tuite, P.J., Gruetter, R., 2006. Proton MRS of the unilateral substantia nigra in the human brain at 4 Tesla: detection of high GABA concentrations. Magn. Reson. Med. 55, 296–301.
Oz, G., Hutter, D., Tkác, I., Clark, H.B., Gross, M.D., Jiang, H., Eberly, L.E., Bushara, K.O., Gomez, C.M., 2010a. Neurochemical alterations in spinocerebellar ataxia type 1 and their correlations with clinical status. Mov. Disord. 25, 1253–1261.
Oz, G., Nelson, C.D., Koski, D.M., Henry, P.G., Marjanska, M., Deelchand, D.K., Shanley, R., Eberly, L.E., Orr, H.T., Clark, H.B., 2010b. Noninvasive detection of presymptomatic and progressive neurodegeneration in a mouse model of spinocerebellar ataxia type 1. J. Neurosci. 30, 3831–3838.
Oz, G., Iltis, I., Hutter, D., Thomas, W., Bushara, K.O., Gomez, C.M., 2010c. Distinct neurochemical profiles of spinocerebellar ataxias 1, 2, 6, and cerebellar multiple system atrophy. Cerebellum 2010 Sep 14. [Epub ahead of print].
Pan, J.W., Telang, F.W., Lee, J.H., de Graaf, R.A., Rothman, D.L., Stein, D.T., Hetherington, H.P., 2001. Measurement of beta-hydroxybutyrate in acute hyperketonemia in human brain. J. Neurochem. 79, 539–544.

Parsons, M.W., Li, T., Barber, P.A., Yang, Q., Darby, D.G., Desmond, P.M., Gerraty, R.P., Tress, B.M., Davis, S.M., 2000. Combined ^{1}H MR spectroscopy and diffusion-weighted MRI improves the prediction of stroke outcome. Neurology 55, 498–505.

Pellerin, L., Magistretti, P.J., 1994. Glutamate uptake into astrocytes stimulates aerobic glycolysis: a mechanism coupling neuronal activity to glucose utilization. Proc. Natl. Acad. Sci. U.S.A. 91, 10625–10629.

Pereira, A.C., Saunders, D.E., Doyle, V.L., Bland, J.M., Howe, F.A., Griffiths, J.R., Brown, M.M., 1999. Measurement of initial *N*-acetyl aspartate concentration by magnetic resonance spectroscopy and initial infarct volume by MRI predicts outcome in patients with middle cerebral artery territory infarction. Stroke 30, 1577–1582.

Pfefferbaum, A., Adalsteinsson, E., Spielman, D., Sullivan, E.V., Lim, K.O., 1999a. *In vivo* spectroscopic quantification of the *N*-acetyl moiety, creatine, and choline from large volumes of brain gray and white matter: effects of normal aging. Magn. Reson. Med. 41, 276–284.

Pfefferbaum, A., Adalsteinsson, E., Spielman, D., Sullivan, E.V., Lim, K.O., 1999b. In vivo brain concentrations of N-acetyl compounds, creatine, and choline in Alzheimer disease. Arch. Gen. Psychiatry 56, 185–192.

Pfeuffer, J., Tkác, I., Provencher, S.W., Gruetter, R., 1999. Toward an *in vivo* neurochemical profile: quantification of 18 metabolites in short-echo-time ^{1}H NMR spectra of the rat brain. J. Magn. Reson. 141, 104–120.

Pilatus, U., Lais, C., Rochmont Adu, M., Kratzsch, T., Frölich, L., Maurer, K., Zanella, F.E., Lanfermann, H., Pantel, J., 2009. Conversion to dementia in mild cognitive impairment is associated with decline of N-acetylaspartate and creatine as revealed by magnetic resonance spectroscopy. Psychiatry Res. 173, 1–7.

Pioro, E.P., Antel, J.P., Cashman, N.R., Arnold, D.L., 1994. Detection of cortical neuron loss in motor neuron disease by proton magnetic resonance spectroscopic imaging *in vivo*. Neurology 44, 1933–1938.

Pioro, E.P., Wang, Y., Moore, J.K., Ng, T.C., Trapp, B.D., Klinkosz, B., Mitsumoto, H., 1998. Neuronal pathology in the wobbler mouse brain revealed by in vivo proton magnetic resonance spectroscopy and immunocytochemistry. Neuroreport 9, 3041–3046.

Pioro, E.P., Majors, A.W., Mitsumoto, H., Nelson, D.R., Ng, T.C., 1999. ^{1}H-MRS evidence of neurodegeneration and excess glutamate + glutamine in ALS medulla. Neurology 53, 71–79.

Podell, M., Hadjiconstantinou, M., Smith, M.A., Neff, N.H., 2003. Proton magnetic resonance imaging and spectroscopy identify metabolic changes in the striatum in the MPTP feline model of parkinsonism. Exp. Neurol. 179, 159–166.

Pohl, C., Block, W., Karitzky, J., Träber, F., Schmidt, S., Grothe, C., Lamerichs, R., Schild, H., Klockgether, T., 2001. Proton magnetic resonance spectroscopy of the motor cortex in 70 patients with amyotrophic lateral sclerosis. Arch. Neurol. 58, 729–735.

Pouwels, P.J., Frahm, J., 1998. Regional metabolite concentrations in human brain as determined by quantitative localized proton MRS. Magn. Reson. Med. 39, 53–60.

Prichard, J., Rothman, D., Novotny, E., Petroff, O., Kuwabara, T., Avison, M., Howseman, A., Hanstock, C., Shulman, R., 1991. Lactate rise detected by ^{1}H NMR in human visual cortex during physiologic stimulation. Proc. Natl. Acad. Sci. U.S.A. 88, 5829–5831.

Provencher, S.W., 1993. Estimation of metabolite concentrations from localized *in vivo* proton NMR spectra. Magn. Reson. Med. 30, 672–679.

Qiu, S., Li, L., Weeber, E.J., May, J.M., 2007. Ascorbate transport by primary cultured neurons and its role in the neuronal function and protection against excitotoxicity. J. Neurosci. Res. 85, 1046–1056.

Quarles, R.H., Macklin, W.B., Morell, P., 2006. Myelin formation, structure and biochemistry, In: Siegel, G.J., et al. (Ed.), Basic Neurochemistry: Molecular, Cellular, and Medical Aspects, 7th edition. Elsevier, New York, pp. 51–71.

Raman, L., Tkac, I., Ennis, K., Georgieff, M.K., Gruetter, R., Rao, R., 2005. *In vivo* effect of chronic hypoxia on the neurochemical profile of the developing rat hippocampus. Brain Res. Dev. Brain Res. 156, 202–209.

Rao, R., Tkáč, I., Townsend, E.L., Gruetter, R., Georgieff, M.K., 2003. Perinatal iron deficiency alters the neurochemical profile of the developing rat hippocampus. J. Nutr. 133, 3215–3221.

Rao, R., Tkac, I., Townsend, E.L., Ennis, K., Gruetter, R., Georgieff, M.K., 2006. Perinatal iron deficiency predisposes the developing rat hippocampus to greater injury from mild to moderate hypoxia–ischemia. J. Cereb. Blood Flow Metab. 27, 729–740.

Ratering, D., Baltes, C., Nordmeyer-Massner, J., Marek, D., Rudin, M., 2008. Performing of a 200-MHz cryogenic RF probe designed for MRI and MRS of the murine brain. Magn. Reson. Med. 59, 1440–1447.

Rebec, G.V., Pierce, R.C., 1994. A vitamin as neuroregulator: ascorbate release into the extracellular fluid of the brain regulates dopaminergic and glutamatergic transmission. Prog. Neurobiol. 43, 537–565.

Rheims, S., Holmgren, C.D., Chazal, G., Mulder, J., Harkany, T., Zilberter, T., Zilberter, Y., 2009. GABA action in immature neocortical neurons directly depends on the availability of keton bodies. J. Neurochem. 110, 1330–1338.

Rice, M.E., 2000. Ascorbate regulation and its neuroprotective role in the brain. Trends Neurosci. 23, 209–216.

Rose, S.E., de Zubicaray, G.I., Wang, D., Galloway, G.J., Chalk, J.B., Eagle, S.C., Semple, J., Doddrell, D.M., 1999. A 1H MRS study of probable Alzheimer's disease and normal aging: implications for longitudinal monitoring of dementia progression. Magn. Reson. Imaging 17, 291–299.

Rose, S.J., Bushi, M., Nagra, I., Davies, W.E., 2000. Taurine fluxes in insulin dependent diabetes mellitus and rehydration in streptozotocin treated rats. Adv. Exp. Med. Biol. 483, 497–501.

Ross, B., Bluml, S., 2001. Magnetic resonance spectroscopy of the human brain. Anat. Rec. 265, 54–84.

Ross, B.D., Higgins, R.J., Boggan, J.E., Willis, J.A., Knittel, B., Unger, S.W., 1988. Carbohydrate metabolism of the rat C6 glioma. An *in vivo* ^{13}C and *in vitro* ^{1}H magnetic resonance spectroscopy study. NMR Biomed. 1, 20–26.

Sager, T.N., Fink-Jensen, A., Hansen, A.J., 1997. Transient elevation of interstitial *N*-acetylaspartate in reversible global brain ischemia. J. Neurochem. 68, 675–682.

Sanacora, G., Gueorguieva, R., Epperson, C.N., Wu, Y.T., Appel, M., Rothman, D.L., Krystal, J.H., Mason, G.F., 2004. Subtype-specific alterations of gamma-aminobutyric acid and glutamate in patients with major depression. Arch. Gen. Psychiatry 61, 705–713.

Sappey-Marinier, D., Calabrese, G., Fein, G., Hugg, J.W., Biggins, C., Weiner, M.W., 1992. Effect of photic stimulation on human visual cortex lactate and phosphates using 1H and 31P magnetic resonance spectroscopy. J. Cereb. Blood Flow Metab. 12, 584–592.

Saravia, F.E., Revsin, Y., Gonzalez Deniselle, M.C., Gonzalez, S.L., Roig, P., Lima, A., Homo-Delarche, F., De Nicola, A.F., 2002. Increased astrocyte reactivity in the hippocampus of murine models of type 1 diabetes: the nonobese diabetic (NOD) and streptozotocin-treated mice. Brain Res. 957, 345–353.

Sarchielli, P., Pelliccioli, G.P., Tarducci, R., Chiarini, P., Presciutti, O., Gobbi, G., Gallai, V., 2001. Magnetic resonance imaging and 1H-magnetic resonance spectroscopy in amyotrophic lateral sclerosis. Neuroradiology 43, 189–197.

Schneider, E., Glover, G., 1991. Rapid *in vivo* proton shimming. Magn. Reson. Med. 18, 335–347.

Schuff, N., Amend, D.L., Knowlton, R., Norman, D., Fein, G., Weiner, M.W., 1999. Age-related metabolite changes and volume loss in the hippocampus by magnetic resonance spectroscopy and imaging. Neurobiol. Aging 20, 279–285.

Schuff, N., Ezekiel, F., Gamst, A.C., Amend, D.L., Capizzano, A.A., Maudsley, A.A., Weiner, M.W., 2001. Region and tissue differences of metabolites in normally aged brain using multislice ^{1}H magnetic resonance spectroscopic imaging. Magn. Reson. Med. 45, 899–907.

Schuff, N., Capizzano, A.A., Du, A.T., Amend, D.L., O'Neill, J., Norman, D., Kramer, J., Jagust, W., Miller, B., Wolkowitz, O.M., Yaffe, K., Weiner, M.W., 2002. Selective reduction of N-acetylaspartate in medial temporal and parietal lobes in AD. Neurology 58, 928–935.

Seaquist, E.R., Damberg, G.S., Tkac, I., Gruetter, R., 2001. The effect of insulin on *in vivo* cerebral glucose concentrations and rates of glucose transport/metabolism in humans. Diabetes 50, 2203–2209.

Selkoe, D.J., 1995. Deciphering Alzheimer's disease: molecular genetics and cell biology yield major clues. J. NIH Res. 7, 57–64.

Server, A., Kulle, B., Gadmar, O.B., Josefsen, R., Kumar, T., Nakstad, P.H., 2010. Measurements of diagnostic examination performance using quantitative apparent diffusion coefficient and proton MR spectroscopic imaging in the preoperative evaluation of tumor grade in cerebral gliomas. Eur. J. Radiol. 2010 Aug 12. [Epub ahead of print].

Shave, E., Pliss, L., Lawrance, M.L., FitzGibbon, T., Stastny, F., Balcar, V.J., 2001. Regional distribution and pharmacological characteristics of [^{3}H]*N*-acethyl-aspartyl-glutamate (NAAG) binding sites in rat brain. Neurochem Int 38, 53–62.

Shen, J., Rothman, D.L., Hetherington, H.P., Pan, J.W., 1999. Linear projection method for automatic slice shimming. Magn. Reson. Med. 42, 1082–1088.

Shirayama, Y., Obata, T., Nonaka, H., Matsuzawa, D., Kanazawa, Y., Yoshitome, E., Ikehira, H., Hashimoto, K., Iyo, M., 2010. Specific metabolites in the medial prefrontal cortex are associated with the neurocognitive deficits in schizophrenia: a preliminary study. Neuroimage 49 (3), 2783–2790.

Sibtain, N.A., Howe, F.A., Saunders, D.E., 2007. The clinical value of proton magnetic resonance spectroscopy in adult brain tumours. Clin. Radiol. 62, 109–119.

Simister, R.J., McLean, M.A., Barker, G.J., Duncan, J.S., 2003. A proton magnetic resonance spectroscopy study of metabolites in the occipital lobes in epilepsy. Epilepsia 44, 550–558.

Simões, R.V., García-Martín, M.L., Cerdán, S., Arús, C., 2008. Perturbation of mouse glioma MRS pattern by induced acute hyperglycemia. NMR Biomed. 21, 251–264.

Simões, R.V., Delgado-Goñi, T., Lope-Piedrafita, S., Arús, C., 2010. ^{1}H-MRSI pattern perturbation in a mouse glioma: the effects of acute hyperglycemia and moderate hypothermia. NMR Biomed. 23, 23–33.

Sivák, S., Bittšanský, M., Kurča, E., Turčanová-Koprušáková, M., Grofik, M., Nosál', V., Poláček, H., Dobrota, D., 2010. Proton magnetic resonance spectroscopy in patients with early stages of amyotrophic lateral sclerosis. Neuroradiology 52, 1079–1085.

Skerritt, J.H., Johnston, G.A., 1982. Postnatal development of GABA binding sites and their endogenous inhibitors in rat brain. Dev. Neurosci. 5, 189–197.

Slotboom, J., Boesch, C., Kreis, R., 1998. Verstile frequency domain fitting using time domain models and prior knowledge. Magn. Reson. Med. 39, 899–911.

Storey, E., Hyman, B.T., Jenkins, B., Brouillet, E., Miller, J.M., Rosen, B.R., Beal, M.F., 1992. 1-Methyl-4-phenylpyridinium produces excitotoxic lesions in rat striatum as a result of impairment of oxidative metabolism. J. Neurochem. 58, 1975–1978.

Suhy, J., Miller, R.G., Rule, R., Schuff, N., Licht, J., Dronsky, V., Gelinas, D., Maudsley, A.A., Weiner, M.W., 2002. Early detection and longitudinal changes in amyotrophic lateral sclerosis by ^{1}H MRSI. Neurology 58, 773–779.

Tate, A.R., Underwood, J., Acosta, D.M., Julià-Sapé, M., Majós, C., Moreno-Torres, A., Howe, F.A., van der Graaf, M., Lefournier, V., Murphy, M.M., Loosemore, A., Ladroue, C., Wesseling, P., Luc Bosson, J., Cabañas, M.E., Simonetti, A.W., Gajewicz, W., Calvar, J., Capdevila, A., Wilkins, P.R., Bell, B.A., Rémy, C., Heerschap, A., Watson, D., Griffiths, J.R., Arús, C., 2006. Development of a decision support system for diagnosis and grading of brain tumours using in vivo magnetic resonance single voxel spectra. NMR Biomed. 19, 411–434.

Taylor-Robinson, S.D., Turjanski, N., Bhattacharya, S., Seery, J.P., Sargentoni, J., Brooks, D.J., Bryant, D.J., Cox, I.J., 1999. A proton magnetic resonance spectroscopy study of the striatum and cerebral cortex in Parkinson's disease. Metab. Brain Dis. 14, 45–55.

Tayoshi, S.Y., Sumitani, S., Taniguchi, K., Shibuya-Tayoshi, S., Numata, S., Iga, J., Nakataki, M., Ueno, S., Harada, M., Ohmori, T., 2009. Metabolite changes and gender differences in schizophrenia using 3-Tesla proton magnetic resonance spectroscopy (^{1}H-MRS). Schizophr. Res. 108, 69–77.

Tedeschi, G., Litvan, I., Bonavita, S., Bertolino, A., Lundbom, N., Patronas, N.J., Hallett, M., 1997. Proton magnetic resonance spectroscopic imaging in progressive supranuclear palsy, Parkinson's disease and corticobasal degeneration. Brain 120, 1541–1552.
Terpstra, M., Gruetter, R., 2004. ^{1}H NMR detection of vitamin C in human brain *in vivo*. Magn. Reson. Med. 51, 225–229.
Terpstra, M., Gruetter, R., High, W.B., Mescher, M., DelaBarre, L., Merkle, H., Garwood, M., 1998a. Lactate turnover in rat glioma measured by *in vivo* nuclear magnetic resonance spectroscopy. Cancer Res. 58, 5083–5088.
Terpstra, M., Anderson, P., Gruetter, 1998b. Localized eddy current compensation using quantitative field mapping. J. Magn. Reson. 131, 139–143.
Terpstra, M., Ugurbil, K., Gruetter, R., 2002. Direct *in vivo* measurement of human cerebral GABA concentration using MEGA-editing at 7 Tesla. Magn. Reson. Med. 47, 1009–1012.
Terpstra, M., Henry, P.G., Gruetter, R., 2003. Measurement of reduced glutathione (GSH) in human brain using LCModel analysis of difference-edited spectra. Magn. Reson. Med. 50, 19–23.
Terpstra, M., Vaughan, T.J., Ugurbil, K., Lim, K.O., Schulz, S.C., Gruetter, R., 2005. Validation of glutathione quantitation from STEAM spectra against edited 1H NMR spectroscopy at 4 T: application to schizophrenia. MAGMA 18, 276–282.
Terpstra, M., Tkác, I., Rao, R., Gruetter, R., 2006. Quantification of vitamin C in the rat brain *in vivo* using short echo-time 1H MRS. Magn. Reson. Med. 55, 979–983.
Terpstra, M., Rao, R., Tkac, I., 2010. Region-specific changes in ascorbate concentration during rat brain development quantified by *in vivo* ^{1}H NMR spectroscopy. NMR Biomed. 23, 1038–1043.
Tkác, I., Henry, P.G., Andersen, P., Keene, C.D., Low, W.C., Gruetter, R., 2004. Highly resolved *in vivo* ^{1}H NMR spectroscopy of the mouse brain at 9.4 T. Magn. Reson. Med. 52, 478–484.
Tkáč, I., Starcuk, Z., Choi, I.Y., Gruetter, R., 1999. *In vivo* ^{1}H NMR spectroscopy of rat brain at 1 ms echo time. Magn. Reson. Med. 41, 649–656.
Tkáč, I., Rao, R., Georgieff, M.K., Gruetter, R., 2003. Developmental and regional changes in the neurochemical profile of the rat brain determined by *in vivo* ^{1}H NMR spectroscopy. Magn. Reson. Med. 50, 24–32.
Tkáč, I., Dubinsky, J.M., Keene, C.D., Gruetter, R., Low, W.C., 2007. Neurochemical changes in Huntington R6/2 mouse striatum detected by *in vivo* ^{1}H NMR spectroscopy. J. Neurochem. 100, 1397–1406.
Tkáč, I., Oz, G., Adriany, G., Uğurbil, K., Gruetter, R., 2009. *In vivo* ^{1}H NMR spectroscopy of the human brain at high magnetic fields: metabolite quantification at 4 T *vs*. 7 T. Magn. Reson. Med. 62, 868–879.
Trachtman, H., Futterweit, S., Sturman, J.A., 1992. Cerebral taurine transport is increased during streptozocin-induced diabetes in rats. Diabetes 41, 1130–1140.
Tsai, M.J., Goh, C.C., Wan, Y.L., Chang, C., 1997. Metabolic alterations produced by 3-nitropropionic acid in rat striata and cultured astrocytes: quantitative *in vitro* ^{1}H nuclear magnetic resonance spectroscopy and biochemical characterization. Neuroscience 79, 819–826.
Turner, R., Chapman, B., Howseman, A.M., Ordidge, R.J., Coxon, R., Glover, P., Mansfield, 1988. Snap-shot magnetic resonance imaging at 0.1 T using double-screened gradients. J. Magn. Reson. 80, 248–258.
Turner, O., Phoenix, J., Wray, S., 1994. Developmental and gestational changes of phosphoethanolamine and taurine in rat brain, striated and smooth muscle. Exp. Physiol. 79, 681–689.
Tveden-Nyborg, P., Johansen, L.K., Raida, Z., Villumsen, C.K., Larsen, J.O., Lykkesfeldt, J., 2009. Vitamin C deficiency in early postnatal life impairs spatial memory and reduces the number of hippocampal neurons in guinea pigs. Am. J. Clin. Nutr. 90, 540–546.
van de Looij, Y., Chatagner, A., Hüppi, P.S., Gruetter, R., Sizonenko, S.V., 2011a. Longitudinal MR assessment of hypoxic ischemic injury in the immature rat brain. Magn. Reson. Med. 65, 305–312.
van de Looij, Y., Kunz, N., Huppi, P., Gruetter, R., Sizonenko, S., 2011b. Diffusion tensor echo planar imaging using surface coil transceiver with a semiadiabatic RF pulse sequence at 14.1 T. Magn. Reson. Med. 65, 732–737.
Van de Moortele, P.F., Akgun, C., Adriany, G., Moeller, S., Ritter, J., Collins, C.M., Smith, M.B., Vaughan, J.T., Ugurbil, K., 2005. B_1 destructive interferences and spatial phase patterns at 7 T with a head transceiver array coil. Magn. Reson. Med. 54, 1503–1518.
van Der Graaf, M., Janssen, S.W., van Asten, J.J., Hermus, A.R., Sweep, C.G., Pikkemaat, J.A., Martens, G.J., Heerschap, A., 2004. Metabolic profile of the hippocampus of Zucker Diabetic Fatty rats assessed by *in vivo* ^{1}H magnetic resonance spectroscopy. NMR Biomed. 17, 405–410.
Van der Veen, J.W., de Beer, R., Luyten, P.R., van Ormondt, D., 1988. Accurate quantification of *in vivo* ^{31}P MRS NMR signals using the variable projection method and prior knowledge. Magn. Reson. Med. 6, 92–98.
Van Vaals, J.J., Bergman, A.H., 1990. Optimization of eddy-current compensation. J. Magn. Reson. 90, 52–70.
Vanhamme, L., Van den Boogaart, A., Van Huffel, S., 1997. Improved method for accurate and efficient quantification fMRS data with use of prior knowledge. J. Magn. Reson. 129, 35–43.
Vannucci, S.J., Seaman, L.B., Brucklacher, R.M., Vannucci, R.C., 1994. Glucose transport in developing rat brain: glucose transporter proteins, rate constants and cerebral glucose utilization. Mol. Cell. Biochem. 140, 177–184.
Verbalis, J.G., 2010. Brain volume regulation in response to changes in osmolality. Neuroscience 168(4):862-70.
Viau, M., Marchand, L., Bard, C., Boulanger, Y., 2005. 1H magnetic resonance spectroscopy of autosomal ataxias. Brain Res. 1049, 191–202.
Wang, S., Poptani, H., Woo, J.H., Desiderio, L.M., Elman, L.B., McCluskey, L.F., Krejza, J., Melhem, E.R., 2006. Amyotrophic lateral sclerosis: diffusion-tensor and chemical shift MR imaging at 3.0 T. Radiology 239, 831–838.
Waniewski, R.A., Martin, D.L., 1998. Preferential utilization of acetate by astrocytes is attributable to transport. J. Neurosci. 18, 5225–5233.
Wardlaw, J.M., Marshall, I., Wild, J., Dennis, M.S., Cannon, J., Lewis, S.C., 1998. Studies of acute ischemic stroke with proton magnetic resonance spectroscopy: relation between time from onset, neurological deficit, metabolite abnormalities in the infarct, blood flow, and clinical outcome. Stroke 29, 1618–1624.
Watanabe, T., Shiino, A., Akiguchi, I., 2010. Absolute quantification in proton magnetic resonance spectroscopy is useful to differentiate amnesic mild cognitive impairment from Alzheimer's disease and healthy aging. Dement Geriatr Cogn Disord 30 (1), 71–77.
Weiss, K., Melkus, G., Jakob, P.M., Faber, C., 2009. Quantitative *in vivo* ^{1}H spectroscopic imaging of metabolites in the early postnatal mouse brain at 17.6 T. MAGMA 22, 53–62.
Westbrook, G.L., Mayer, M.L., Namboodiri, M.A., Neale, J.H., 1986. High concentrations of *N*-acethylaspartylglutamate (NAAG) selectively activate NMDA receptors on mouse spinal cord neurons in cell culture. J. Neurosci. 6, 3385–3392.
Wijnen, J.P., Scheenen, T.W., Klomp, D.W., Heerschap, A., 2010a. ^{31}P magnetic resonance spectroscopic imaging with polarisation transfer of phosphomono- and diesters at 3 T in the human brain: relation with age and spatial differences. NMR Biomed. 23, 968–976.
Wijnen, J.P., Van der Graaf, M., Scheenen, T.W., Klomp, D.W., de Galan, B.E., Idema, A.J., Heerschap, A., 2010b. *In vivo* ^{13}C magnetic resonance spectroscopy of a human brain tumor after application of ^{13}C-1-enriched glucose. Magn. Reson. Imaging 28, 690–697.
Wright, A.C., Song, H.K., Wehrili, F.W., 2000. *In vivo* MR micro imaging with conventional radiofrequency coils cooled to 77 degree K. Magn. Reson. Med. 43, 163–169.
Xin, L., Gambarota, G., Mlynárik, V., Gruetter, R., 2008. Proton T2 relaxation time of J-coupled cerebral metabolites in rat brain at 9.4 T. NMR Biomed. 21, 396–401.
Xin, L., Gambarota, G., Duarte, J.M.N., Mlynárik, V., Gruetter, R., 2010a. Direct *in vivo* measurement of glycine and the neurochemical profile in the rat medulla oblongata. NMR Biomed. 23, 1097–1102.
Xin, L., Mlynárik, V., Lanz, B., Frenkel, H., Gruetter, R., 2010b. ^{1}H-[^{13}C] NMR spectroscopy of the rat brain during infusion of [2-^{13}C] acetate at 14.1 T. Magn. Reson. Med. 64, 334–340.
Xu, S., Yang, J., Li, C.Q., Zhu, W., Shen, J., 2005. Metabolic alterations in focally activated primary somatosensory cortex of alpha-chloralose-anesthetized rats measured by ^{1}H MRS at 11.7 T. Neuroimage 28, 401–409.
Yang, J., Shen, J., 2006. Increased oxygen consumption in the somatosensory cortex of alpha-chloralose anesthetized rats during forepaw stimulation determined using MRS at 11.7 Tesla. Neuroimage 32, 1317–1325.
Yao, F.S., Caserta, M.T., Wyrwicz, A.M., 1999. *In vitro* proton and phosphorus NMR spectroscopic analysis of murine (C57Bl/6J) brain development. NMR Biomed. 12, 463–470.
Yao, J.K., Leonard, S., Reddy, R., 2006. Altered glutathione redox state in schizophrenia. Dis. Markers 22, 83–93.
Yoo, S.Y., Yeon, S., Choi, C.H., Kang, D.H., Lee, J.M., Shin, N.Y., Jung, W.H., Choi, J.S., Jang, D.P., Kwon, J.S., 2009. Proton magnetic resonance spectroscopy in subjects with high genetic risk of schizophrenia: investigation of anterior cingulate, dorsolateral prefrontal cortex and thalamus. Schizophr. Res. 111, 86–93.
Yoon, J.H., Maddock, R.J., Rokem, A., Silver, M.A., Minzenberg, M.J., Ragland, J.D., Carter, C.S., 2010. GABA concentration is reduced in visual cortex in schizophrenia and correlates with orientation-specific surround suppression. J. Neurosci. 30, 3777–3781.
Zacharoff, L., Tkac, I., Song, Q., Tang, C., Bolan, P.J., Mangia, S., Henry, P.G., Li, T., Dubinsky, J.M., 2011. Cortical metabolites as biomarkers in the R6/2 model of Huntington's disease. J Cereb Blood Flow Metab. 2011 Nov 2. doi:10.1038/jcbfm.2011.157. [Epub ahead of print].
Zand, D.J., Simon, E.M., Pulitzer, S.B., Wang, D.J., Wang, Z.J., Rorke, L.B., Palmieri, M., Berry, G.T., 2003. *In vivo* pyruvate detected by MR spectroscopy in neonatal pyruvate dehydrogenase deficiency. AJNR Am. J. Neuroradiol. 24, 1471–1474.
Zhang, Y., Li, S., Shen, J., 2009. Automatic high-order shimming using parallel columns mapping (PACMAP). Magn. Reson. Med. 63, 1073–1079.
Zhao, J., Ramadan, E., Capiello, M., Wroblewska, B., Bzdega, T., Neale, J.H., 2001. NAAG inhibits KCl-induced [^{3}H]-GABA release via mGluR3, cAMP, PKA and L-type calcium conductance. Eur. J. Neurosci. 13, 340–346.
Zwingmann, C., Butterworth, R., 2005. An update of the role of brain glutamine synthesis and its relation to cell-specific energy metabolism in the hyperammonemic brain: further studies using NMR spectroscopy. Neurochem. Int. 47, 19–30.